Fyziologie buň. systému

Aktivace vývojových mechanismů u dospělého organismu

doc. Mgr. Vítězslav Bryja, Ph.D.

Indukované kmenové buňky - iPSCs

Cell

Induction of Pluripotent Stem Cells from Mouse Embryonic and Adult Fibroblast Cultures by Defined Factors

Kazutoshi Takahashi[1] and Shinya Yamanaka[1,2,*]
[1] Department of Stem Cell Biology, Institute for Frontier Medical Sciences, Kyoto University, Kyoto 606-8507, Japan
[2] CREST, Japan Science and Technology Agency, Kawaguchi 332-0012, Japan
*Contact: yamanaka@frontier.kyoto-u.ac.jp
DOI 10.1016/j.cell.2006.07.024

SUMMARY

Differentiated cells can be reprogrammed to an embryonic-like state by transfer of nuclear contents into oocytes or by fusion with embryonic stem (ES) cells. Little is known about factors

or by fusion with ES cells (Cowan et al., 2005; Tada et al., 2001), indicating that unfertilized eggs and ES cells contain factors that can confer totipotency or pluripotency to somatic cells. We hypothesized that the factors that play important roles in the maintenance of ES cell identity also play pivotal roles in the induction of pluripotency in somatic cells.

Indukované kmenové buňky - iPSCs

Oct3/4
Sox2
c-Myc
Klf4

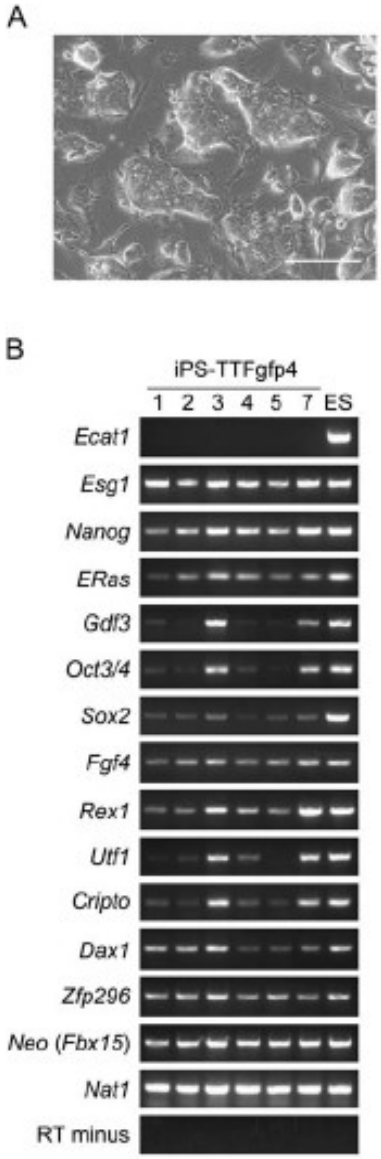

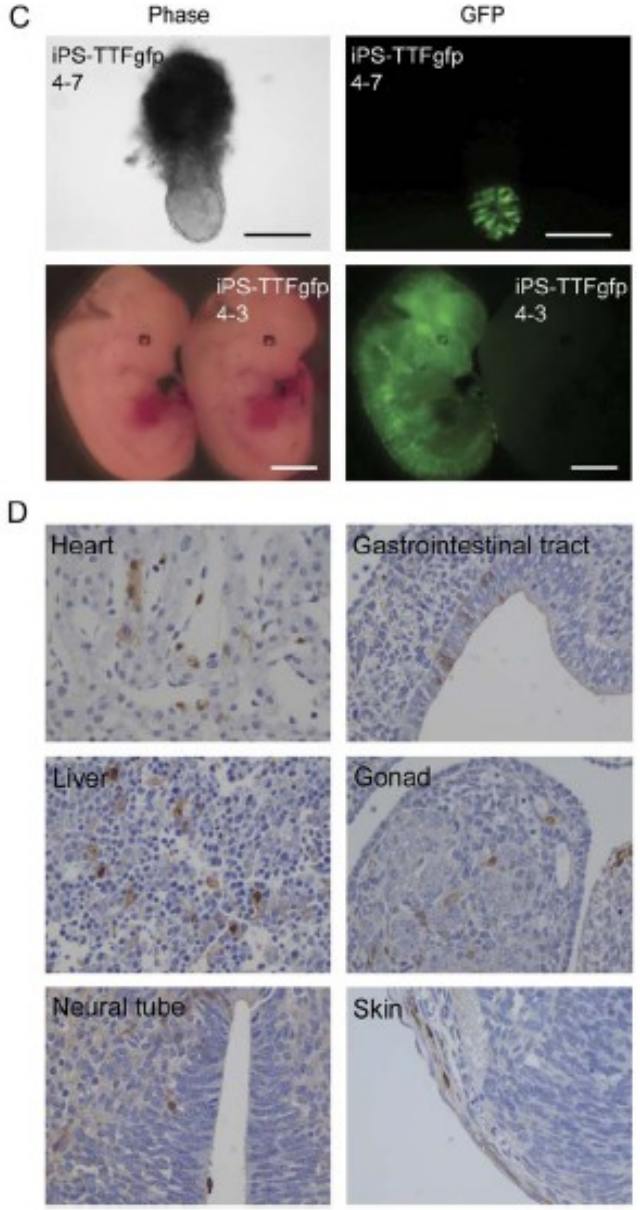

Indukované kmenové buňky - iPSCs

2012 Nobel Prize in Physiology or Medicine

Shinya Yamanaka
University of Kyoto, Japan
Photo Credit:
Center for iPS cell Research and Application, Kyoto University

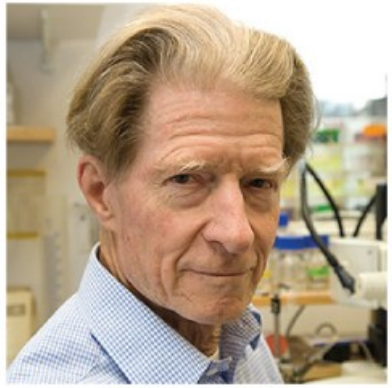

John B. Gurdon
Gurdon Institute in Cambridge, UK

Induced Pluripotent Stem (iPS) Cells

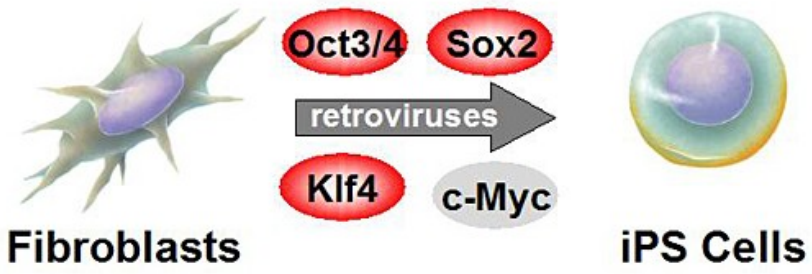

Mouse iPS cells reported in 2006

Human iPS cells reported in 2007

Direct reprogramming – přímé přeprogramování

Proces, kterým lze s použitím kombinace transkripčních faktorů (nebo inhibitorů/aktivátorů signálních drah) změnit jeden buněčný typ v druhý.

ARTICLES

nature biotechnology

Induction of functional dopamine neurons from human astrocytes *in vitro* and mouse astrocytes in a Parkinson's disease model

Pia Rivetti di Val Cervo[1], Roman A Romanov[2,3], Giada Spigolon[3], Débora Masini[3], Elisa Martín-Montañez[1,4], Enrique M Toledo[1], Gioele La Manno[1], Michael Feyder[3], Christian Pifl[2], Yi-Han Ng[5], Sara Padrell Sánchez[1], Sten Linnarsson[1], Marius Wernig[5], Tibor Harkany[2,3], Gilberto Fisone[3] & Ernest Arenas[1]

Cell replacement therapies for neurodegenerative disease have focused on transplantation of the cell types affected by the pathological process. Here we describe an alternative strategy for Parkinson's disease in which dopamine neurons are generated by direct conversion of astrocytes. Using three transcription factors, NEUROD1, ASCL1 and LMX1A, and the microRNA miR218, collectively designated NeAL218, we reprogram human astrocytes *in vitro*, and mouse astrocytes *in vivo*, into induced dopamine

Kmenové buňky

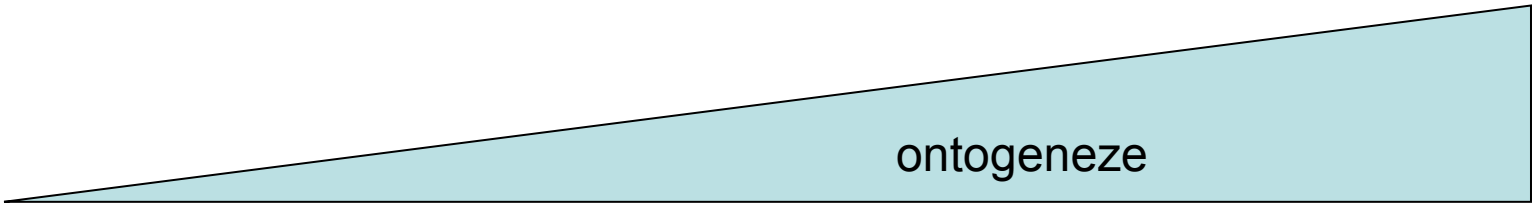

blastocysta

vyvíjející se tkáň (orgán)

dospělá tkáň

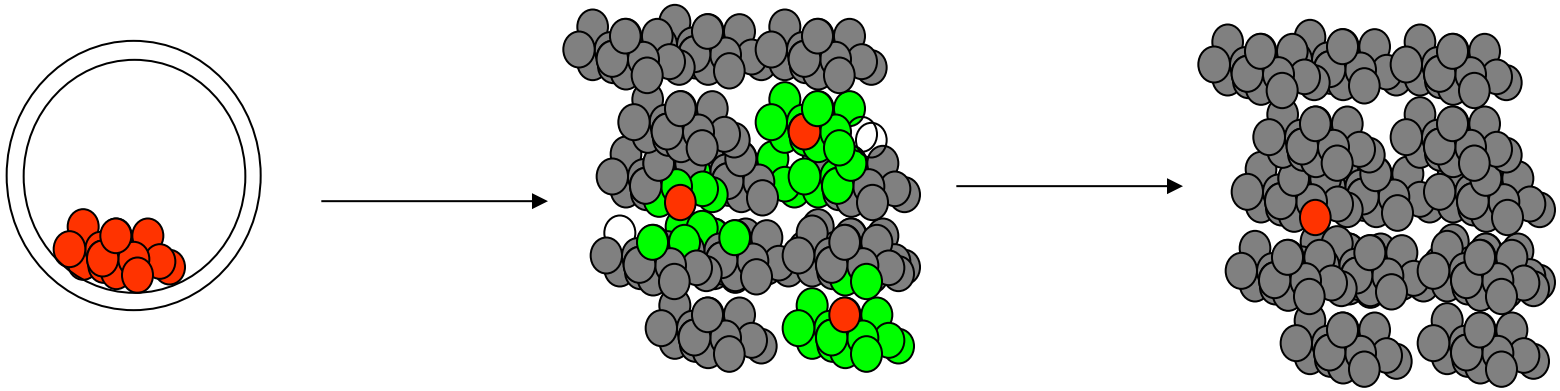

K čemu jsou, jak vypadají a jak jsou regulovány kmenové buňky v dospělém organismu?

K čemu jsou tkáňově specifické kmenové buňky?

1) K zajištění homeostázy

- v lidském organismu běžně regenerují celé tkáně – např. vlasové kořínky (doba „života“ 3-4 roky), epitel střeva, epitel plic, krevní buňky nebo játra

2) K zajištění procesu hojení a regenerace

Časy – délka „života“ buněk

cell type	turnover time	BNID
small intestine epithelium	2–4 days	107812, 109231
stomach	2–9 days	101940
blood neutrophils	1–5 days	101940
white blood cells eosinophils	2–5 days	109901, 109902
gastrointestinal colon crypt cells	3–4 days	107812
cervix	6 days	110321
lungs alveoli	8 days	101940
tongue taste buds (rat)	10 days	111427
platelets	10 days	111407,111408
bone osteoclasts	2 weeks	109906
intestine paneth cells	20 days	107812
skin epidermis cells	10–30 days	109214, 109215
pancreas beta cells (rat)	20–50 days	109228
blood B cells	1 month	111516
trachea	1–2 months	101940
hematopoietic stem cells	2 months	109232
sperm (male gametes)	2 months	110319, 110320
bone osteoblasts	3 months	109907
red blood cells	4 months	101706, 107875
liver hepatocyte cells	0.5–1 year	109233
fat cells	8 years	103455
cardiomyocytes	0.5–10% per year	107076, 107077, 107078
central nervous system	life-time	101940
skeleton	10% per year	109908
lens cells	life-time	109840
oocytes (female gametes)	life-time	111451

Jak zjistit délku „života“ buněk/intenzitu obnovy tkání?

Využití přechodného zvýšení ^{14}C z dob studené války
(Jonas Frisén, Karolinska)

Nervové buňky mozkové kůry

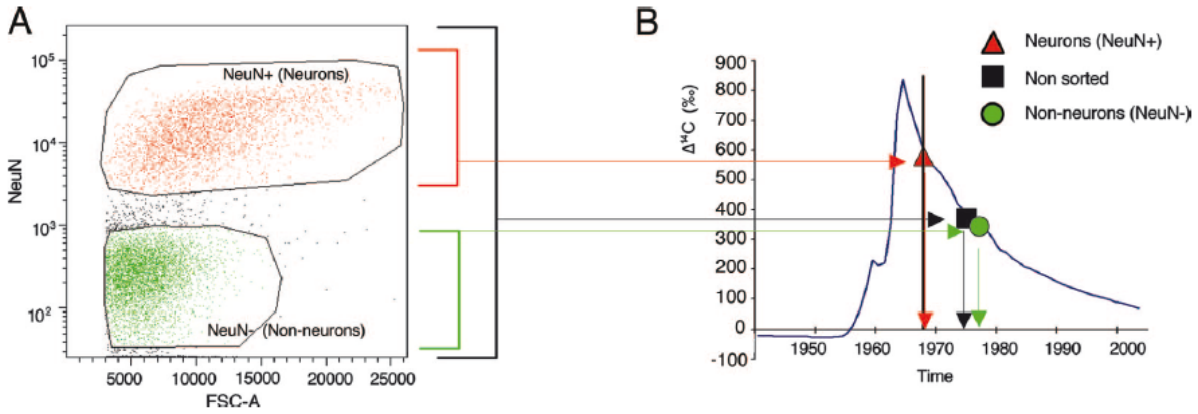

Fig. 1. Determination of the age of neocortical neurons. (*A*) Neuronal (NeuN-positive) and nonneuronal (NeuN-negative) cell nuclei from the adult human cerebral necortex were separated and isolated by flow cytometry. (*B*) The levels of ^{14}C in the atmosphere have been stable over long time periods, with the exception of a large addition of ^{14}C in 1955–1963 as a result of nuclear weapons tests (blue line, data from ref. 26), making it possible to infer the time of birth of cell populations by relating the level of ^{14}C in DNA to that in the atmosphere (horizontal arrows) and reading the age off the *x* axis (vertical arrows). The average age of all cells in the prefrontal cortex is younger than the individual (black arrows), indicating cell turnover. Dating of nonneuronal cells demonstrates they are younger, whereas neurons are approximately as old as the individual. The vertical bar indicates the year of birth of the individual. ^{14}C levels from modern samples are, by convention, given in relation to a universal standard and corrected for radioactive decay, giving the $\Delta^{14}C$ value (50).

Regenerace srdce:

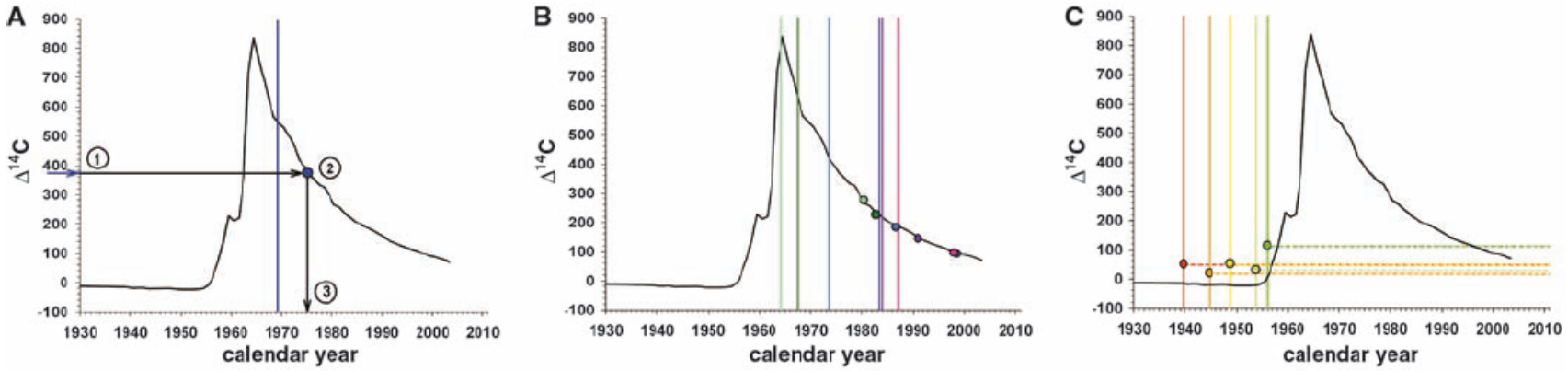

Fig. 1. Cell turnover in the heart. (**A**) Schematic figure demonstrating the strategy to establish cell age by ^{14}C dating. The black curve in all graphs shows the atmospheric concentrations of ^{14}C over the decades since 1930 [data from (*14*)]. The vertical bar indicates the date of birth of the individual. The measured ^{14}C concentration (1) is related to the atmospheric ^{14}C concentration by use of the established atmospheric ^{14}C bomb curve (2). The average birth date of the population can be inferred by determining where the data point intersects the *x* axis (3). ^{14}C concentrations in DNA of cells from the left ventricle myocardium in individuals born after (**B**) or before (**C**) the nuclear bomb tests correspond to time points substantially after the time of birth, indicating postnatal cell turnover. The vertical bar indicates the date of birth of each individual, and the similarly colored dots represent the ^{14}C data for the same individual. For individuals born before the increase in ^{14}C concentrations, it is not possible to directly infer an age because the measured concentration can be a result of ^{14}C incorporation during the rising and/or falling part of the atmospheric curve, and thus the concentration is indicated by a dotted horizontal line.

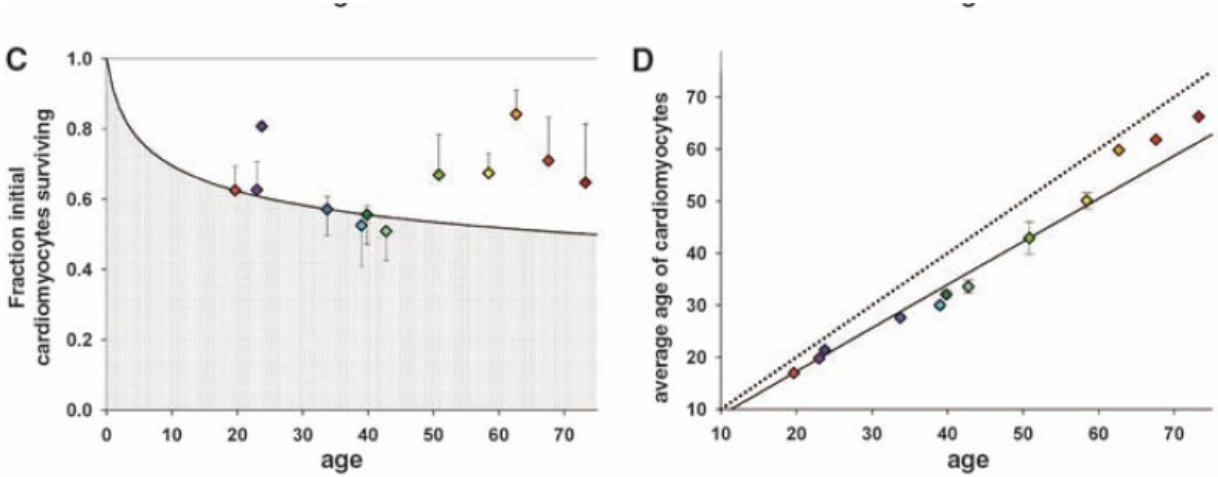

Schopnosti regenerace se liší mezi jednotlivými organismy

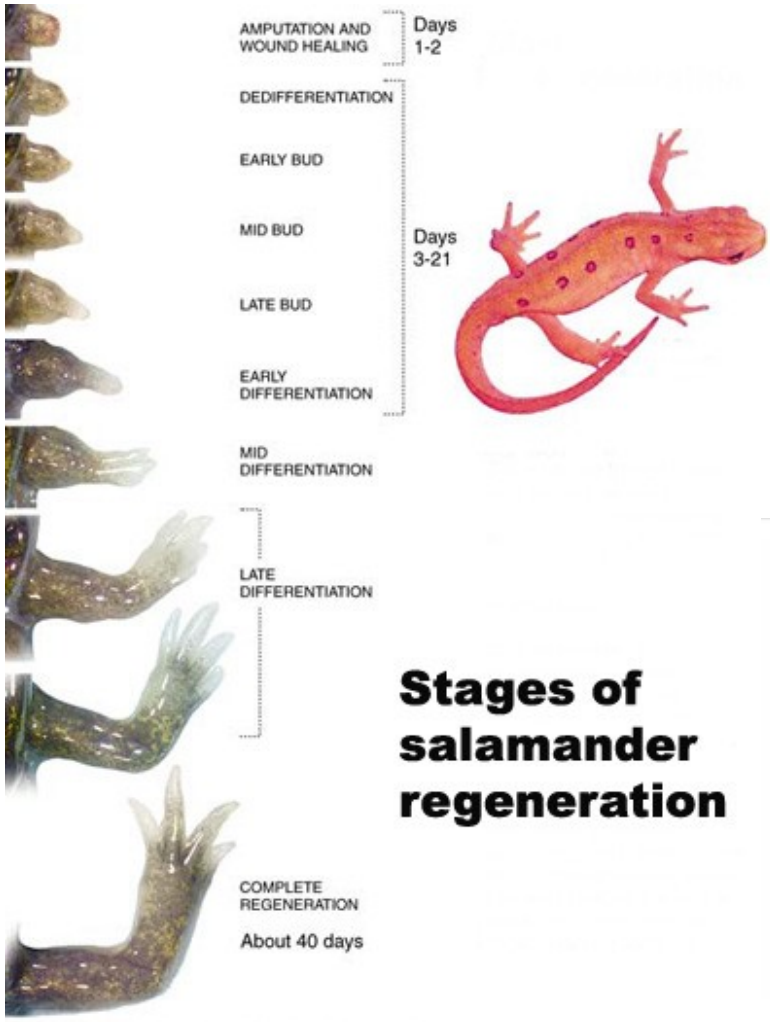

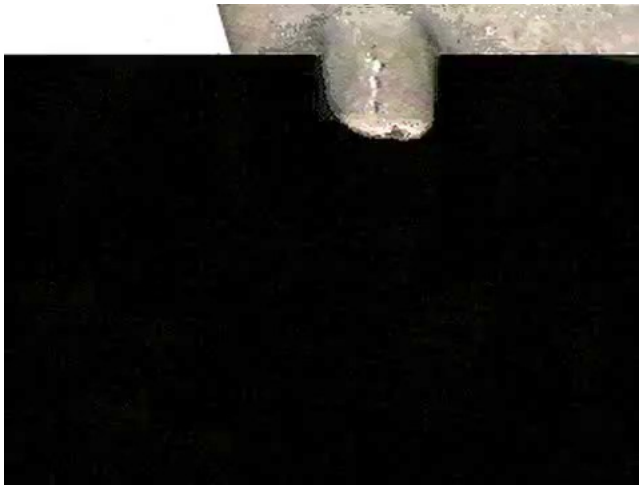

JMG reptile tm

"GECKO TAIL REGENERATION"

Schopnosti regenerace se liší mezi jednotlivými organismy

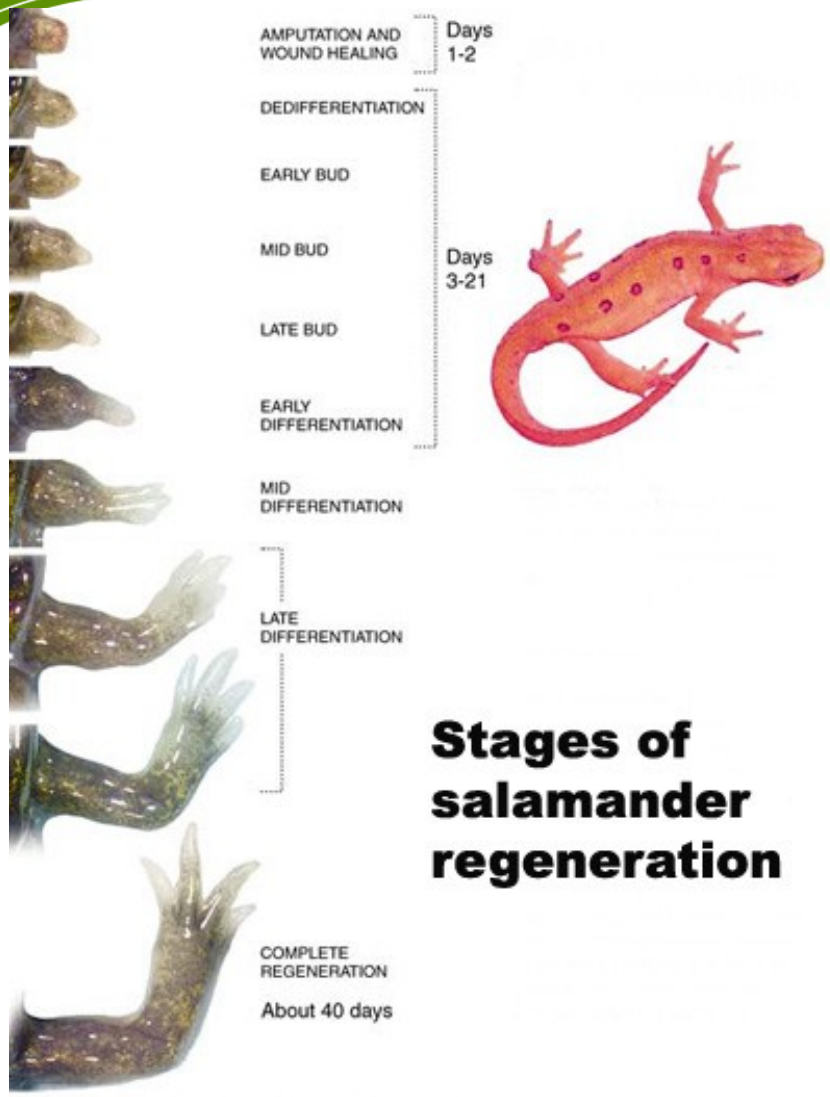

po amputaci:

po 10 letech:

Morfogenetické sign. dráhy (kanonická Wnt signalizace, Hedgehog, TGF, Notch) jsou nezbytné pro regeraci u řady mnohobuněčných organismů

axolotl

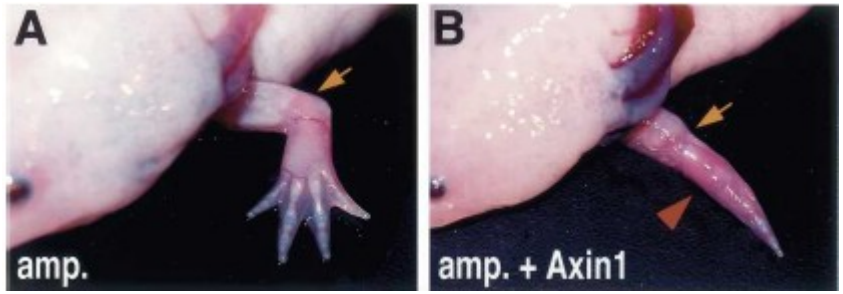

chick

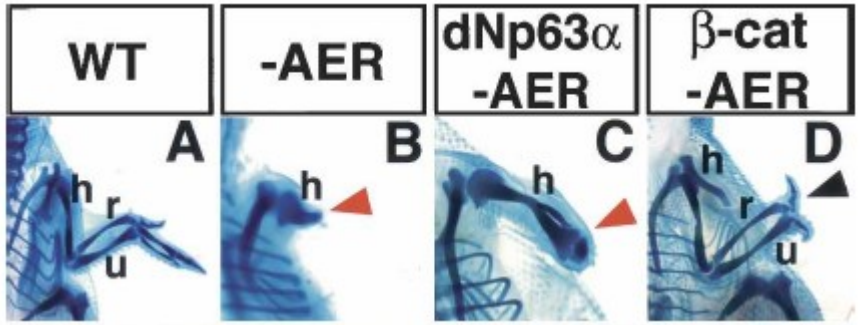

Morfogenetické sign. dráhy (kanonická Wnt signalizace, Hedgehog, TGF, Notch) jsou nezbytné pro regeraci u řady mnohobuněčných organismů

zebrafish

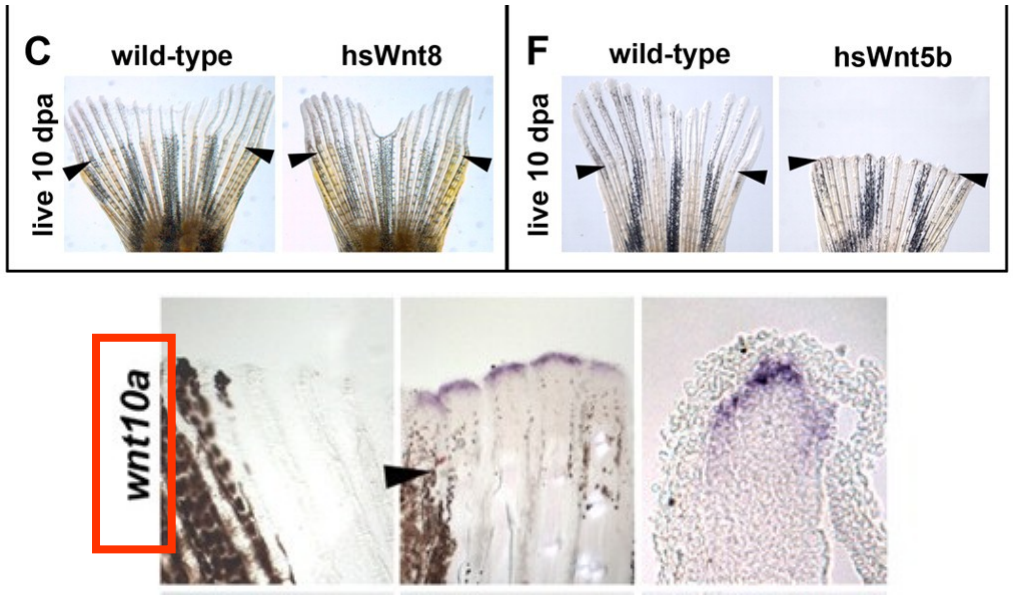

... Regenerace pod kontrolou Wnt signální dráhy u ploštěnky

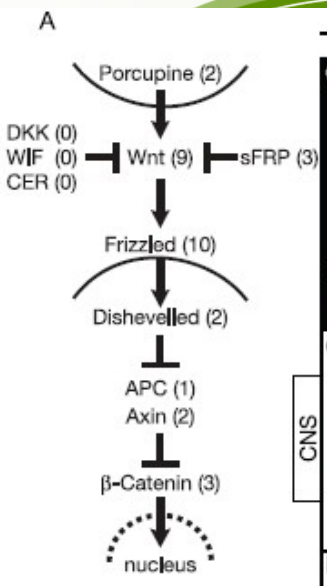

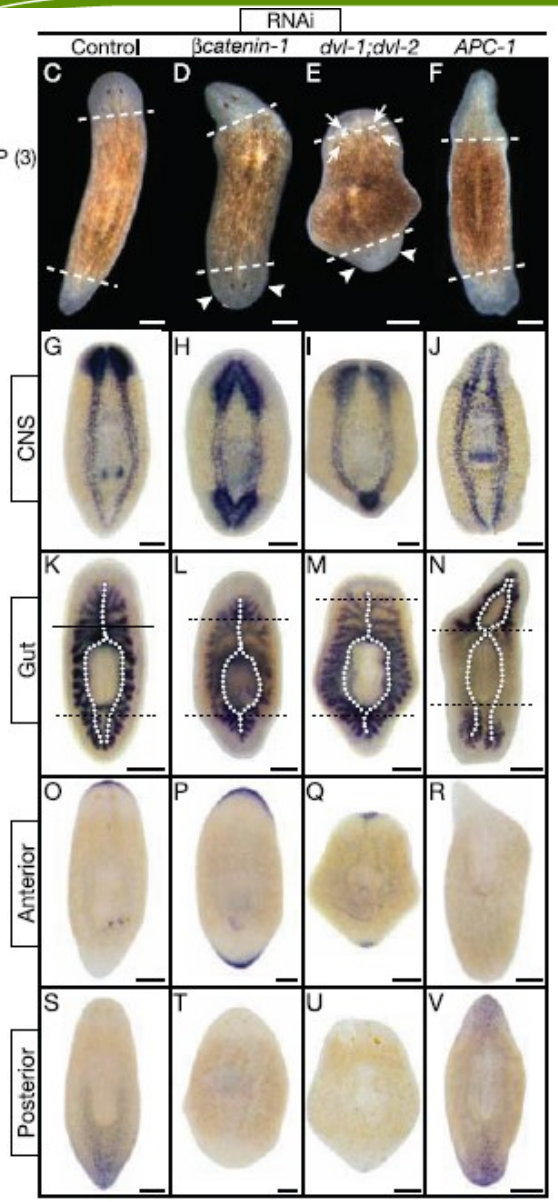

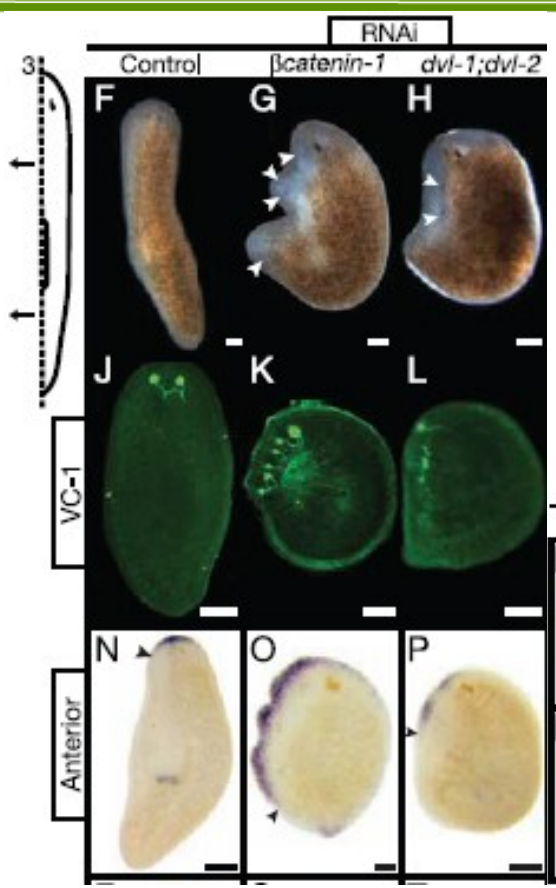

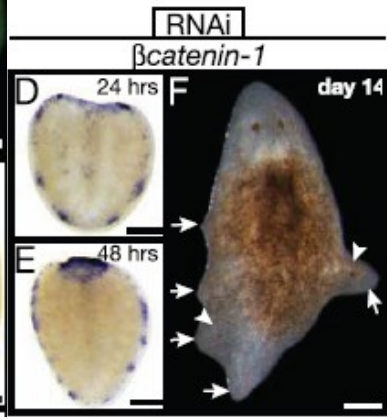

β-Catenin Defines Head Versus Tail Identity During Planarian Regeneration and Homeostasis

Kyle A. Gurley, Jochen C. Rink, Alejandro Sánchez Alvarado*

SCIENCE VOL 319 18 JANUARY 2008

Kde jsou adult stem cells a jak vypadají?

Nika kmenových buněk – stem cell niche

- Kmenové buňky jednotlivých tkání se vzájemně liší – co se týče např. schopnosti proliferovat nebo naopak zůstávat zcela „inaktivní“ (quiescent)
- Kmenové buňky jsou pod kontrolou svého mikroprostředí – tzv. niky kmenových buněk (stem cell niche)
- V biologii kmenových buněk mají zásadní význam dráhy kontrolující embryonální vývoj – např. Wnt, FGF, Hedgehog, Notch atd.
- Kmenové buňky zodpovědné za obměnu tkání v rámci homeostázy se mohou lišit od těch, které se aktivují v procesu regenerace

Prostředí kmenových buněk (stem cell niche)

vlasový kořínek

Figure 4 The hair follicle. Stem cells reside in the bulge niche. Cells can migrate upwards from here to populate the sebaceous gland and the interfollicular epidermis. Cells that migrate downwards enter the matrix where they rapidly proliferate and then differentiate to form the hair. (Adapted from ref. 90.)

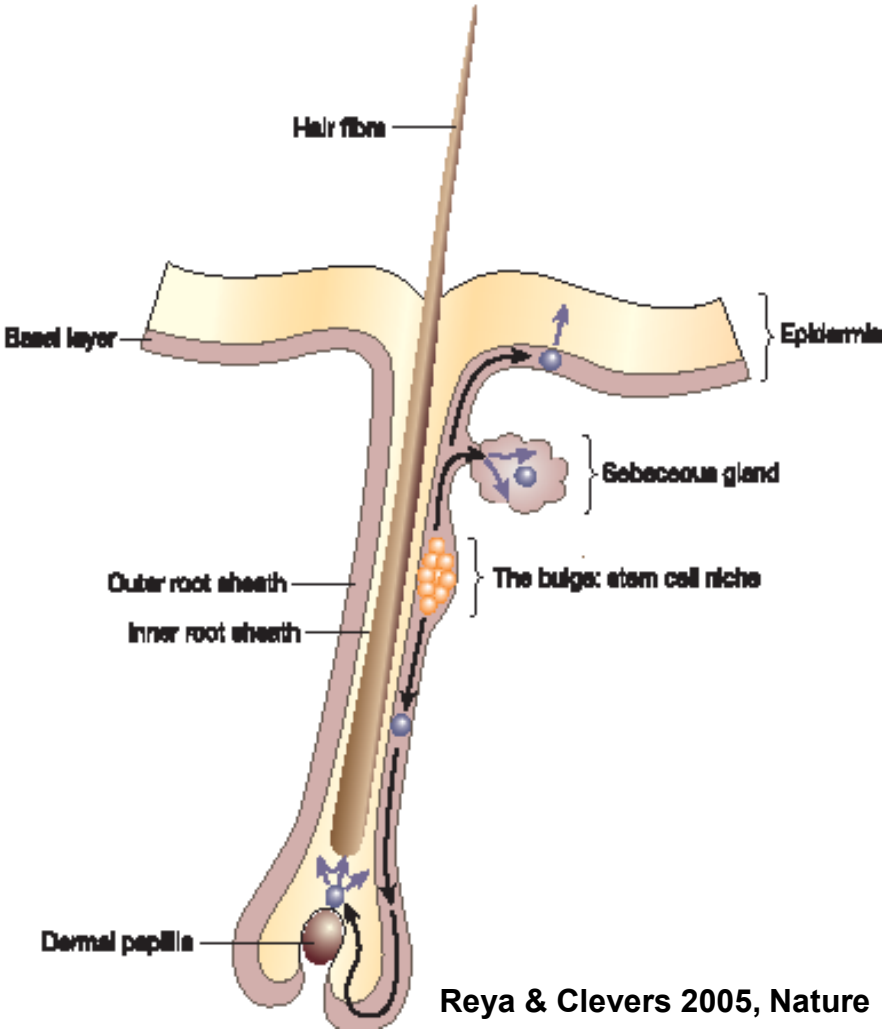

Reya & Clevers 2005, Nature

Prostředí kmenových buněk (stem cell niche)

kostní dřeň

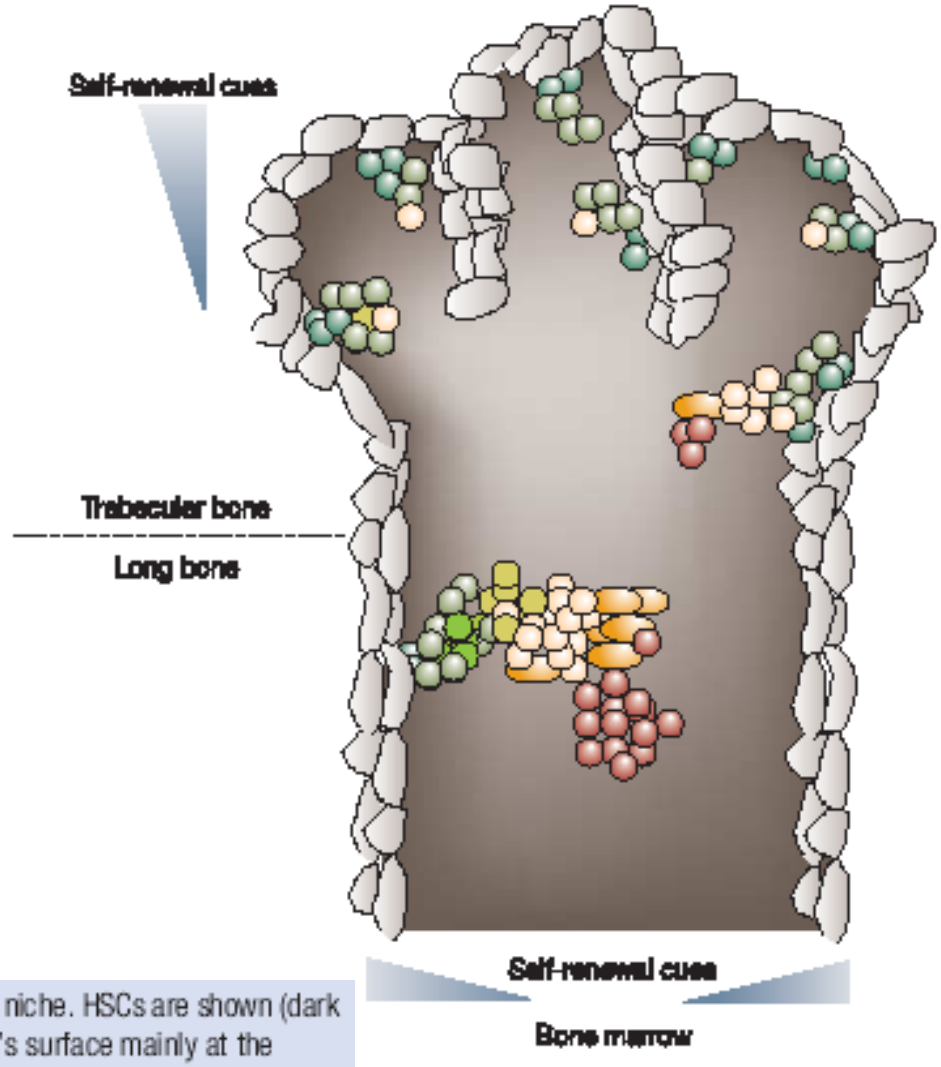

Figure 5 Proposed model of HSC development in the niche. HSCs are shown (dark green) at the endosteal marrow adjacent to the bone's surface mainly at the trabecular bone, and are postulated to migrate inward in the central marrow as they differentiate (precursors in light green; differentiated cells in yellow, orange and red) away from a possible gradient of self-renewal cues. (Adapted from ref. 44.)

Reya & Clevers 2005, Nature

Epitel střeva jako modelový příklad funkce tkáňových buněk a hierarchické organizace tkání

- S využitím klíčových objevů prof. Hanse Cleverse (Utrecht) a jeho animací

Kmenové buňky střevního epitelu

Kmenové buňky střeva (2006)

střevní epitel

2006: kmenové buňky definovány jako „label-retaining cells“

- tj. jako buňky, které se nedělí

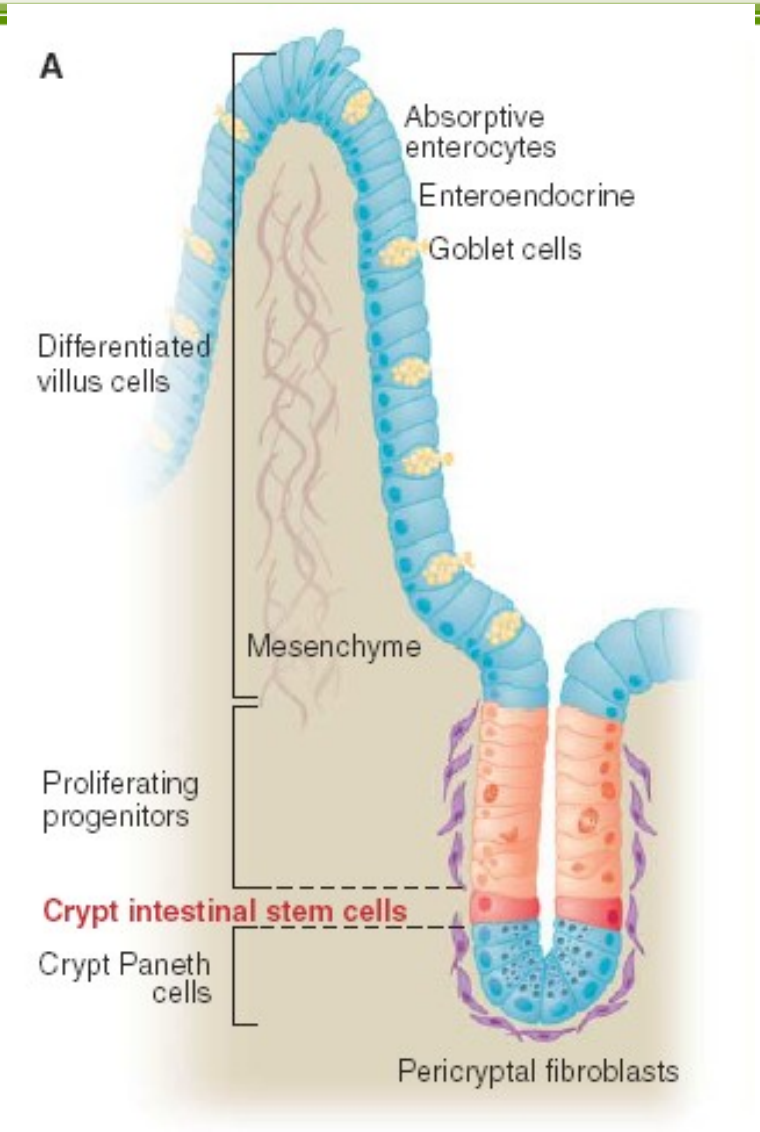

Moore & Lemischka, Science, 2006

Hon za dospělými kmenovými buňkami – Lgr5

střevní epitel – jak prokázat, že je buňka kmenová (Barker et al., Nature, October 2007)

A. Příprava transgenní myši č. 1 za účelem zjistit, kde je nový potenciální stem cell marker exprimován (in vivo expression profiling). Lgr5 je exprimován specificky v buňkách ve spodní části krypty.

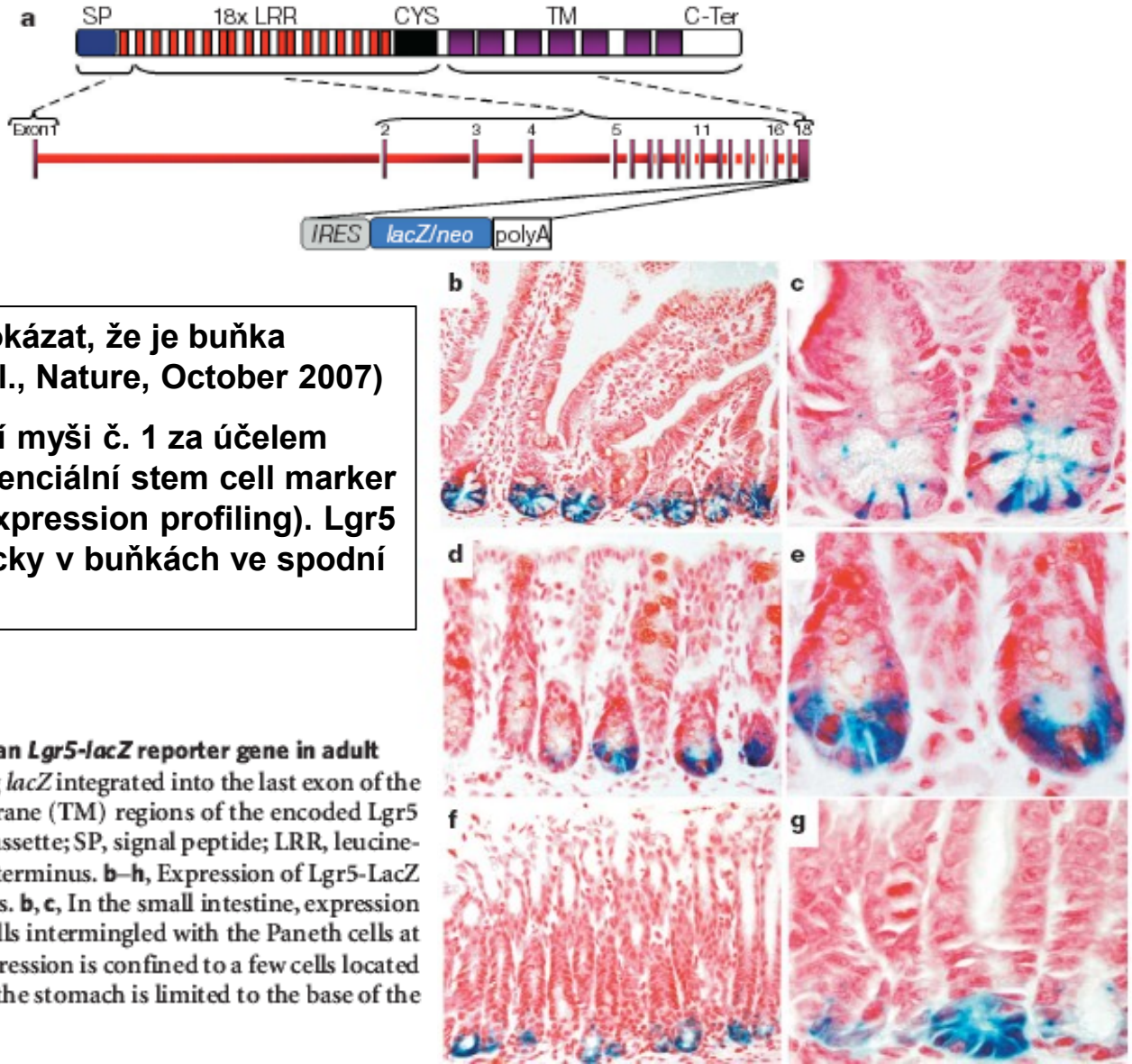

Figure 3 | Restricted expression of an *Lgr5-lacZ* reporter gene in adult mice. **a**, Generation of mice carrying *lacZ* integrated into the last exon of the *Lgr5* gene, removing all transmembrane (TM) regions of the encoded Lgr5 protein. Neo, neomycin resistance cassette; SP, signal peptide; LRR, leucine-rich repeat region; C-Ter is carboxy terminus. **b**–**h**, Expression of Lgr5-LacZ (blue) in selected adult mouse tissues. **b**, **c**, In the small intestine, expression is restricted to six to eight slender cells intermingled with the Paneth cells at the crypt base. **d**, **e**, In the colon, expression is confined to a few cells located at the crypt base. **f**, **g**, Expression in the stomach is limited to the base of the glands.

Hon za dospělými kmenovými buňkami

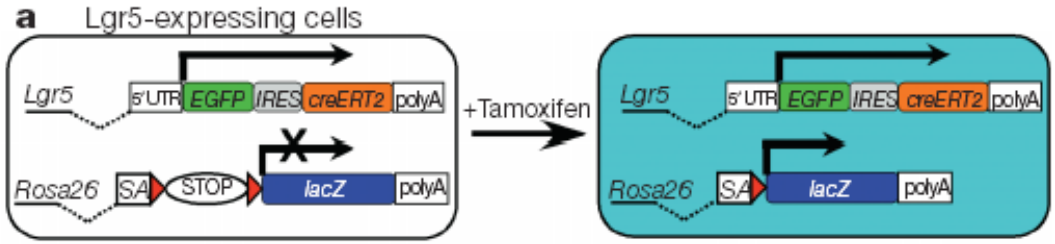

střevní epitel – jak prokázat, že je buňka kmenová (Barker et al., Nature, October 2007)

B. Příprava transgenní myši 2, 3 a 4 za účelem zjistit, co všechno vzniká z Lgr5-pozitivních buněk (Lgr5+ lineage tracing). Lgr5 pozitivní buňky dávají vzniknout všem částem buněčného epitelu.

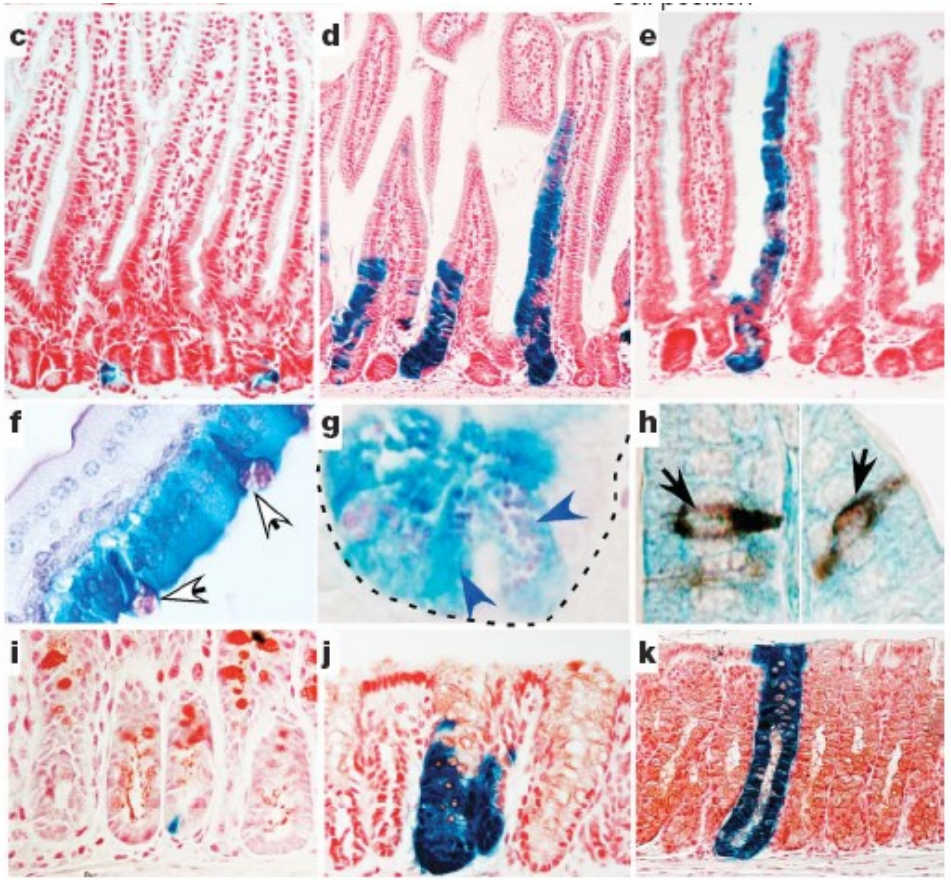

Figure 5 | Lineage tracing in the small intestine and colon. **a**, *Lgr5-EGFP-IRES-creERT2* knock-in mouse crossed with *Rosa26-lacZ* reporter mice 12 h after tamoxifen injection. **b**, Frequency at which the blue cells appeared at carrying activated Cre. **c–e**, Histological analysis of LacZ activity in small intestine 1 day after induction (**c**), 5 days after induction (**d**) and 60 days after induction (**e**). **f–h**, Double-labelling of LacZ-stained intestine using PAS demonstrates the presence of goblet cells (**f**, white arrows) and Paneth cells (**g**, blue arrows) in induced blue clones. Double-labelling with synaptophysin demonstrates the presence of enteroendocrine cells within the induced blue clones (**h**, black arrows). **i–k**, Histological analysis of LacZ activity in colon 1 day after induction (**i**), 5 days after induction (**j**) and 60 days after induction (**k**).

Hon za dospělými kmenovými buňkami

střevní epitel –D. Závěr: Kmenové buňky epitelu tlustého i tenkého střeva jsou protáhlé, dříve nepovšimnuté buňky, v relativní pozici 1´, 2´ a 3´od spodu krypty.

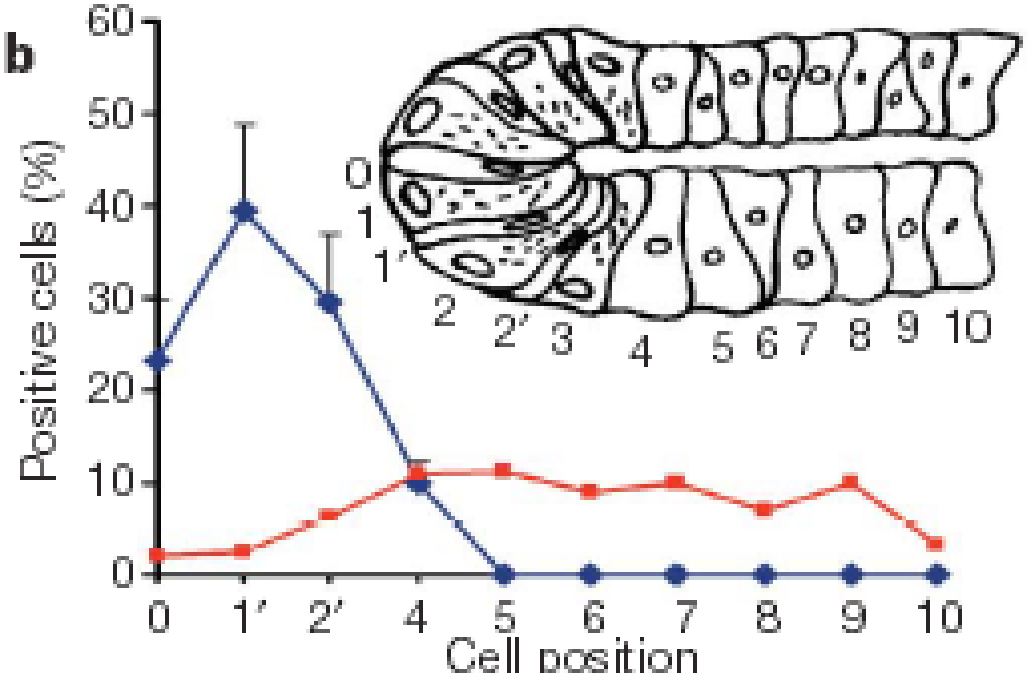

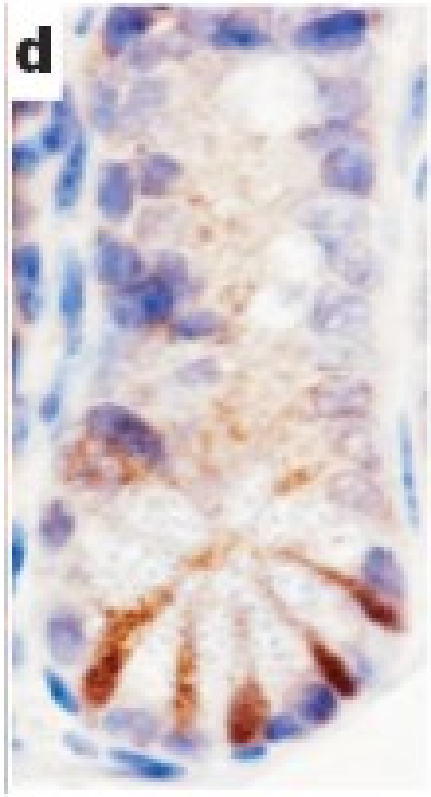

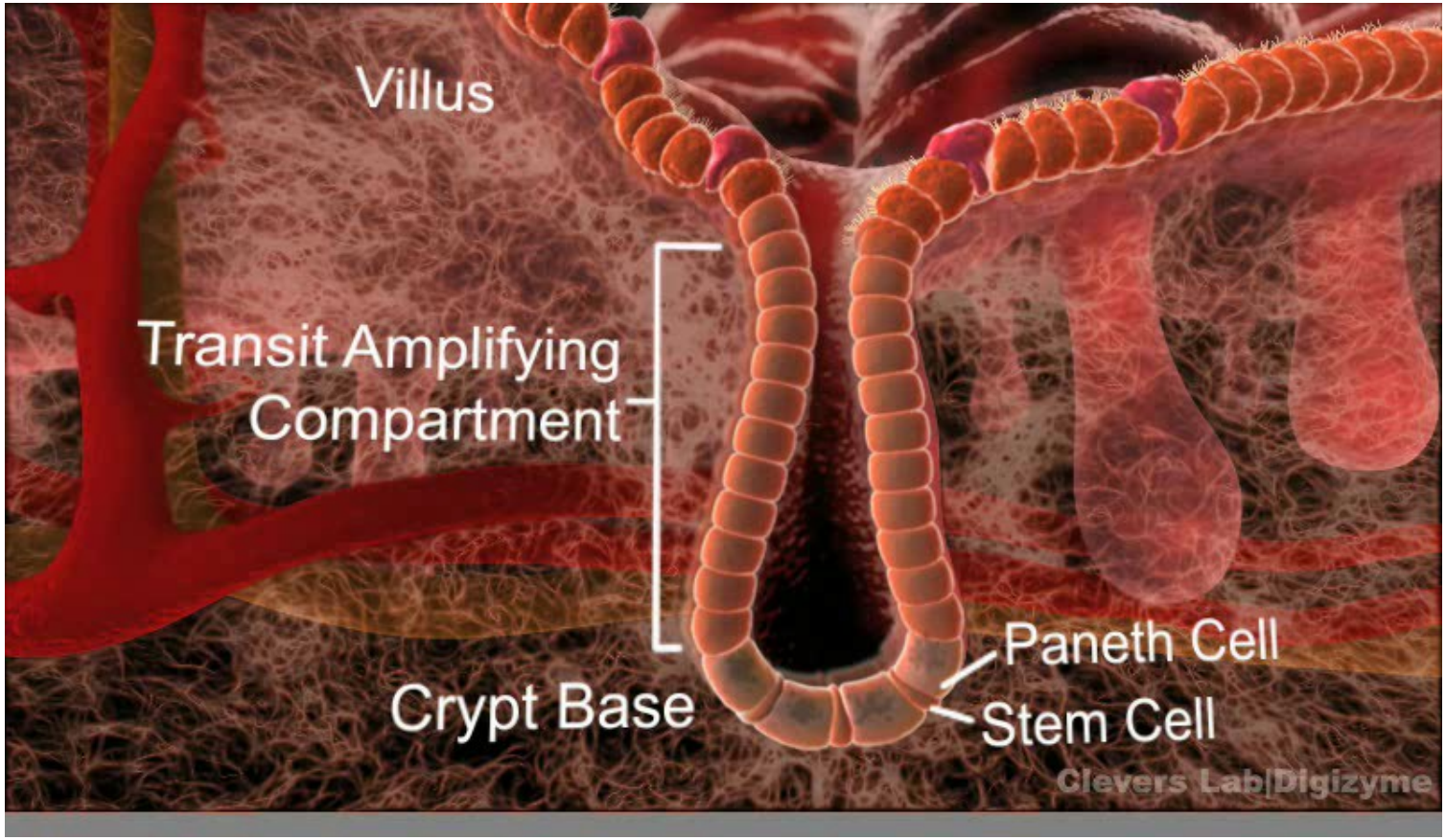
Villus
Transit Amplifying Compartment
Crypt Base
Paneth Cell
Stem Cell
Clevers Lab|Digizyme

Jsou si kmenové buňky rovnocenné a zůstávají stále na stejném místě

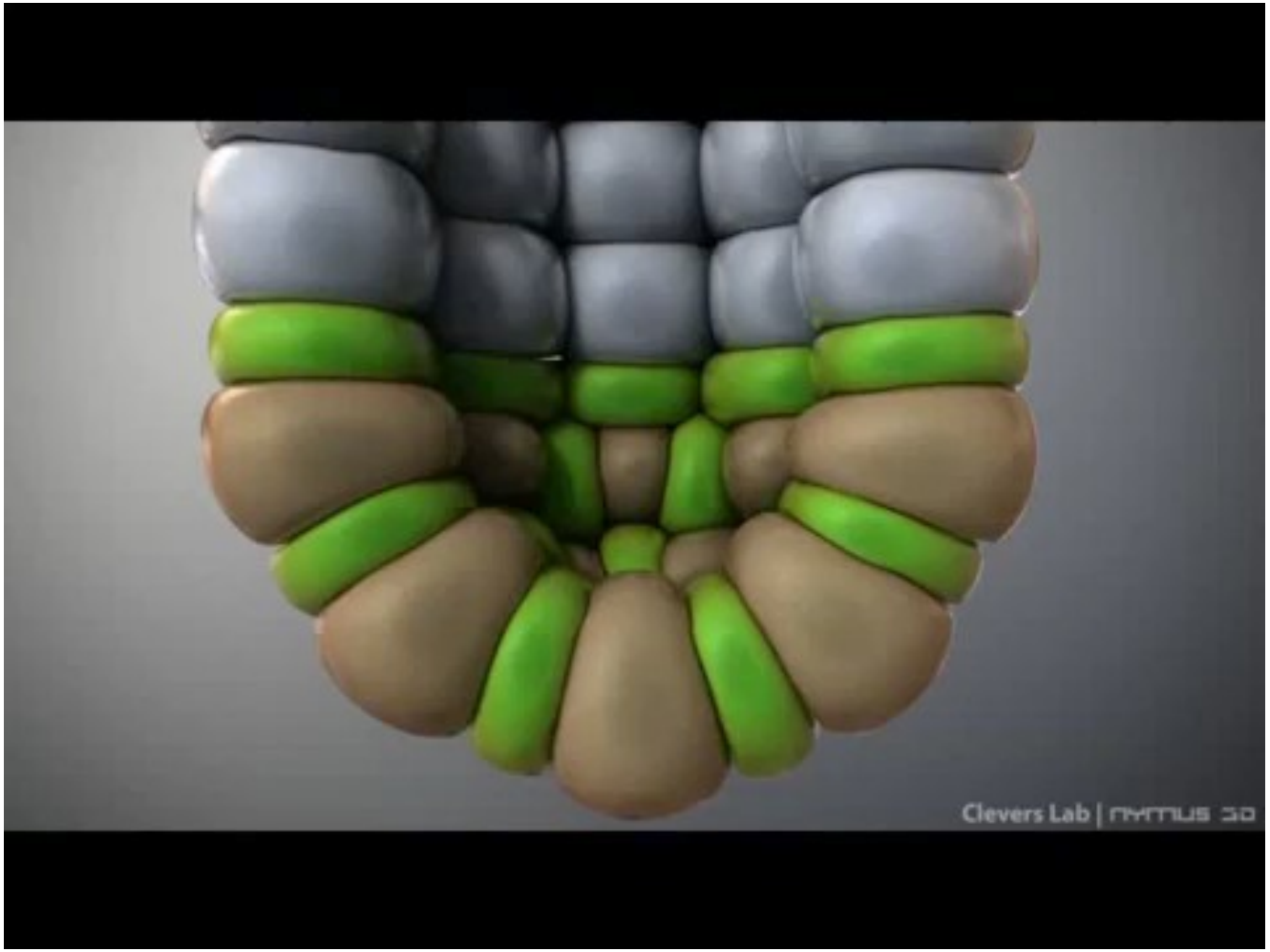

Rosa26 locus in Mouse, Chr6

Cre recombination

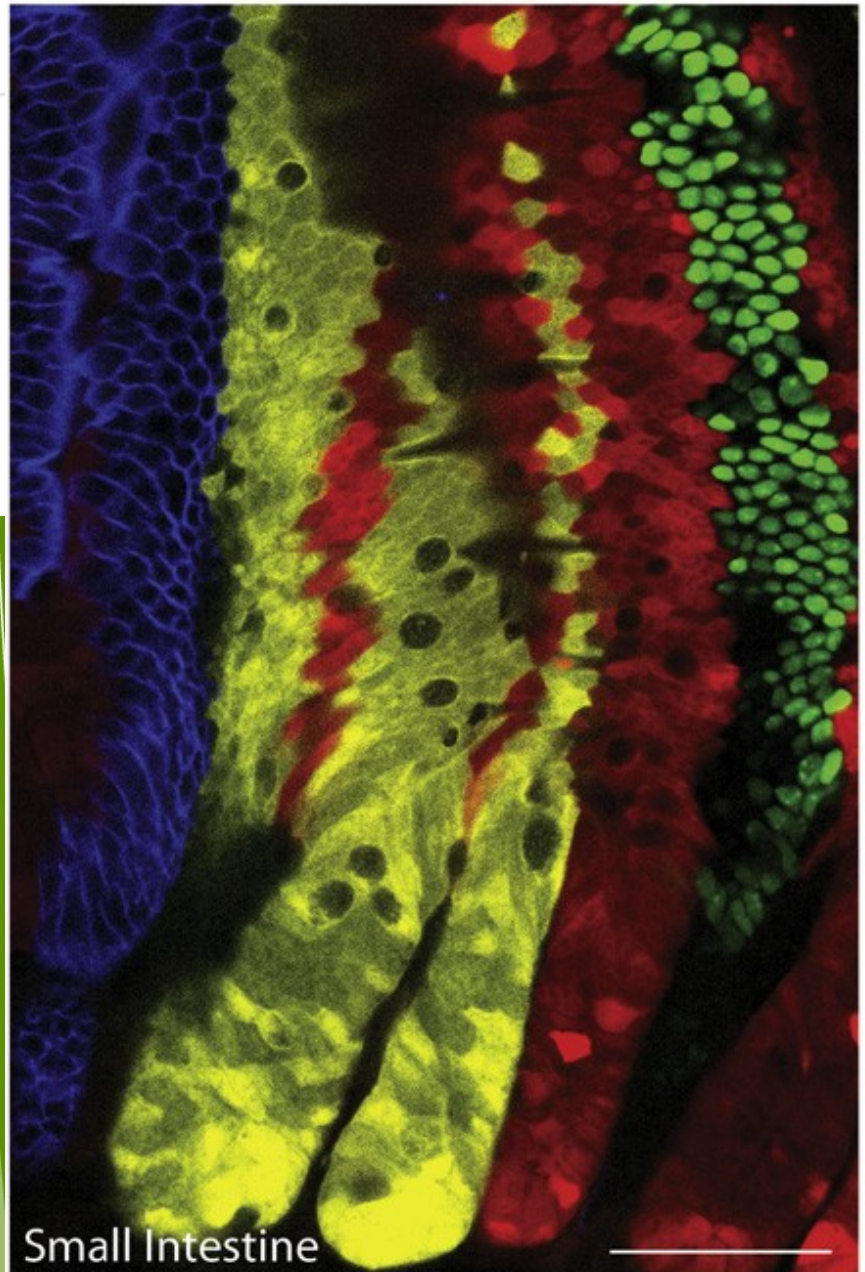

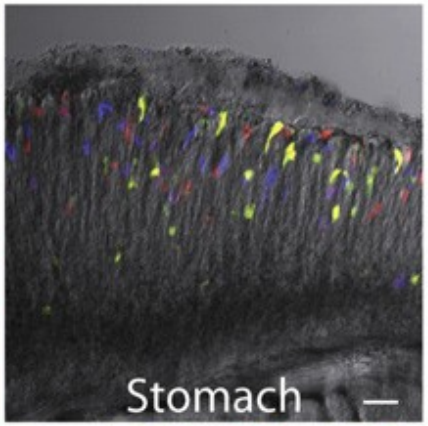

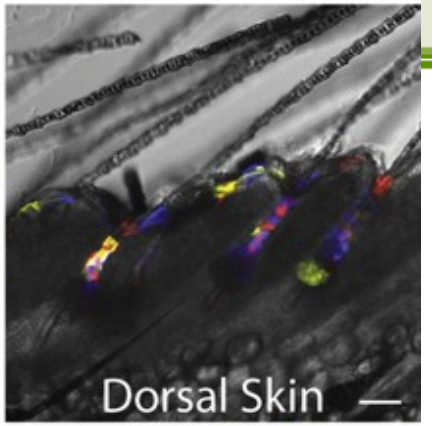

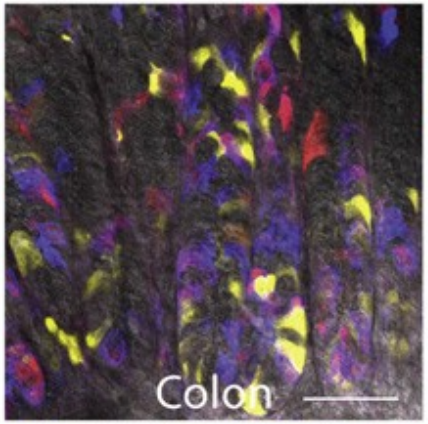

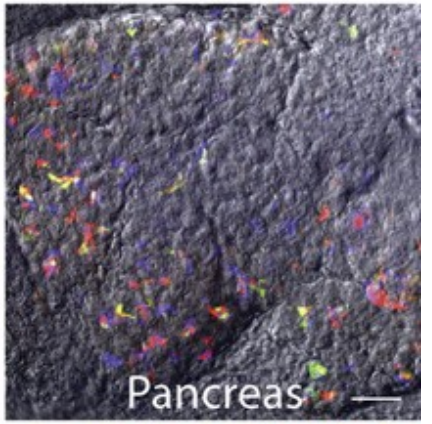

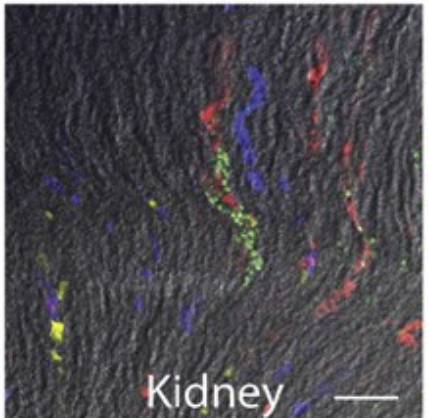

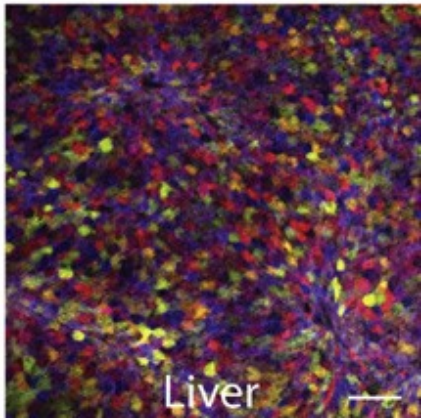

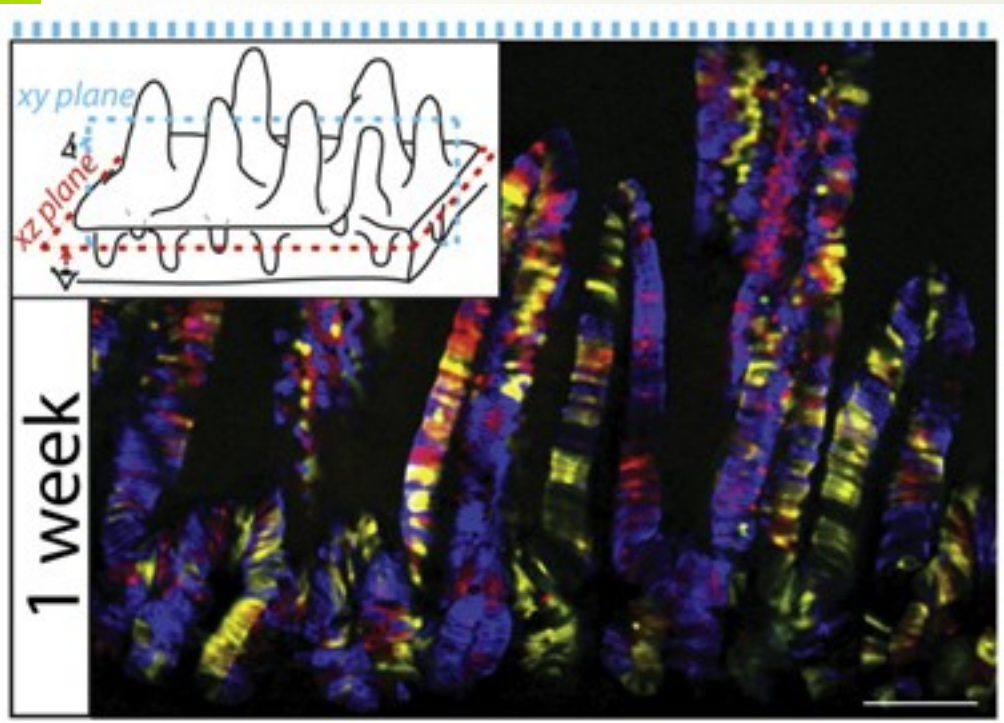

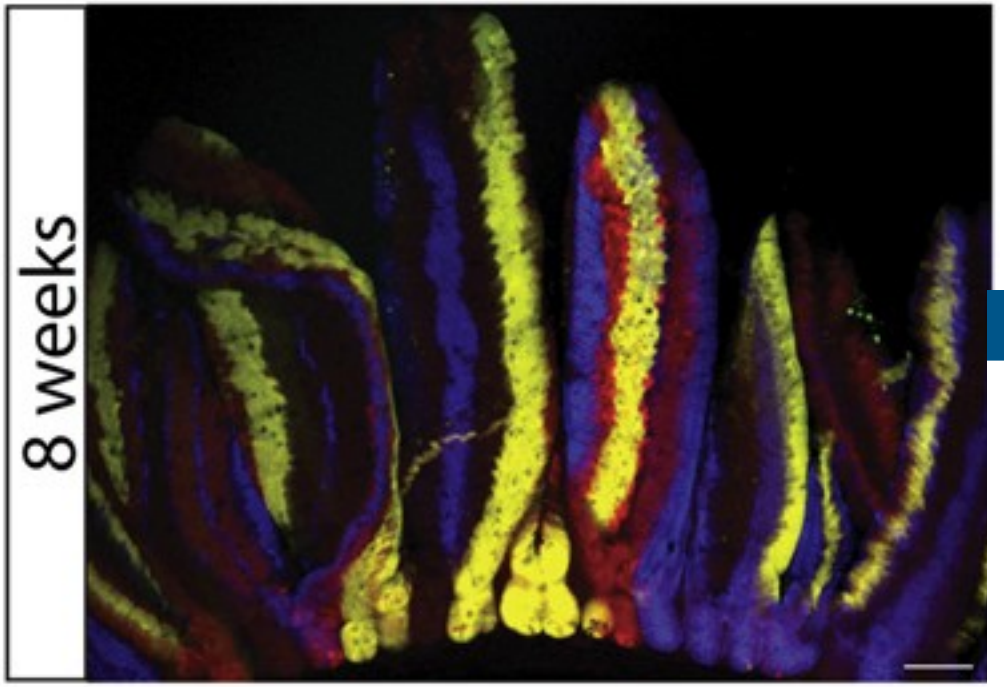

Cell

Intestinal Crypt Homeostasis Results from Neutral Competition between Symmetrically Dividing Lgr5 Stem Cells

Hugo J. Snippert,[1] Laurens G. van der Flier,[1] Toshiro Sato,[1] Johan H. van Es,[1] Maaike van den Born,[1] Carla Kroon-Veenboer,[1] Nick Barker,[1] Allon M. Klein,[2,3] Jacco van Rheenen,[1] Benjamin D. Simons,[3] and Hans Clevers[1,*]
[1]Hubrecht Institute, KNAW and University Medical Center Utrecht, Uppsalalaan 8, 3584 CT Utrecht, The Netherlands
[2]Department of Systems Biology, Harvard Medical School, 200 Longwood Avenue, Boston, MA 02115, USA
[3]Department of Physics, Cavendish Laboratory, J.J. Thomson Avenue, Cambridge CB3 0HE, UK
*Correspondence: h.clevers@hubrecht.eu
DOI 10.1016/j.cell.2010.09.016

Stem cell competition - movie

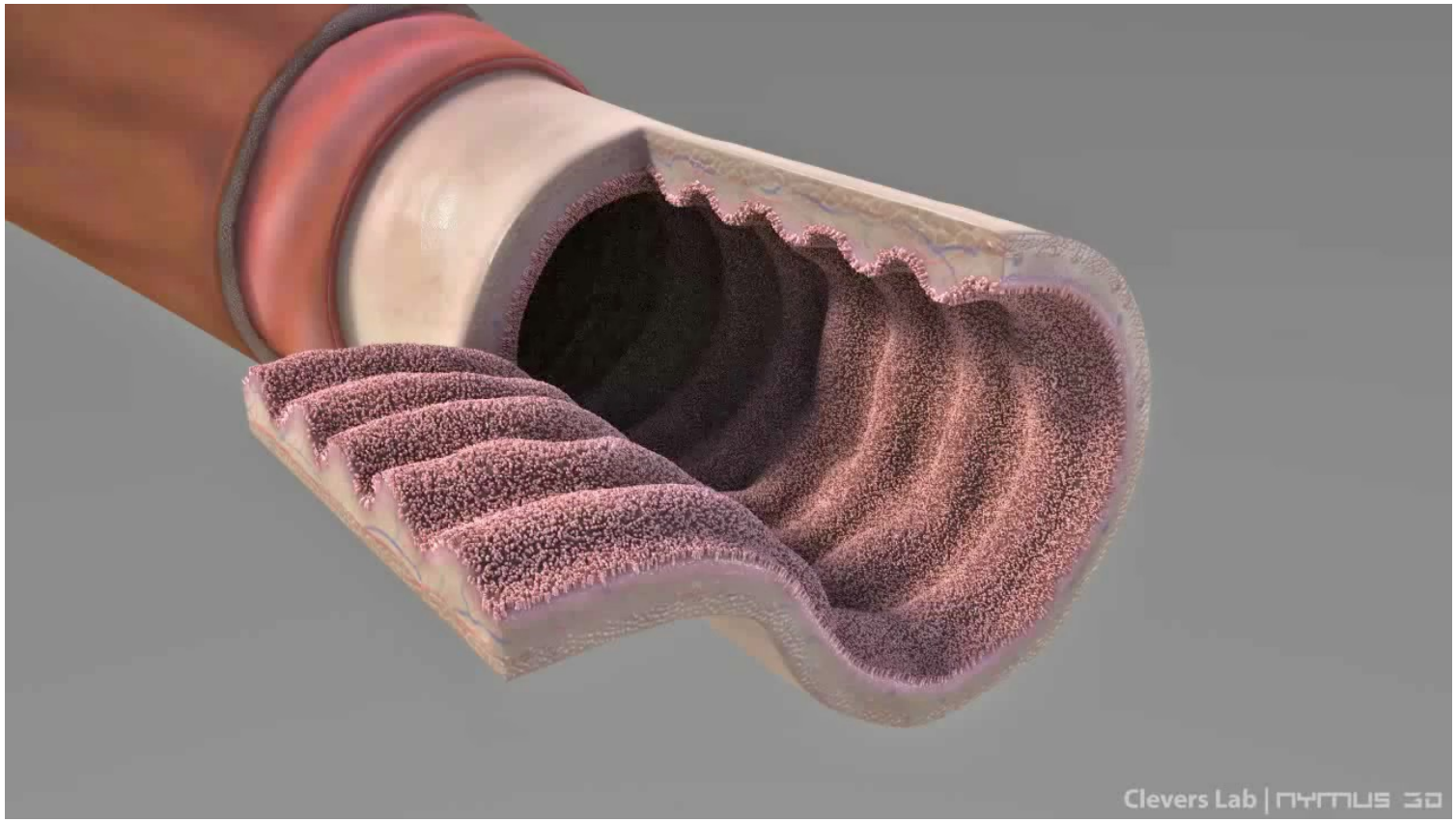

Prostředí kmenových buněk (stem cell niche)

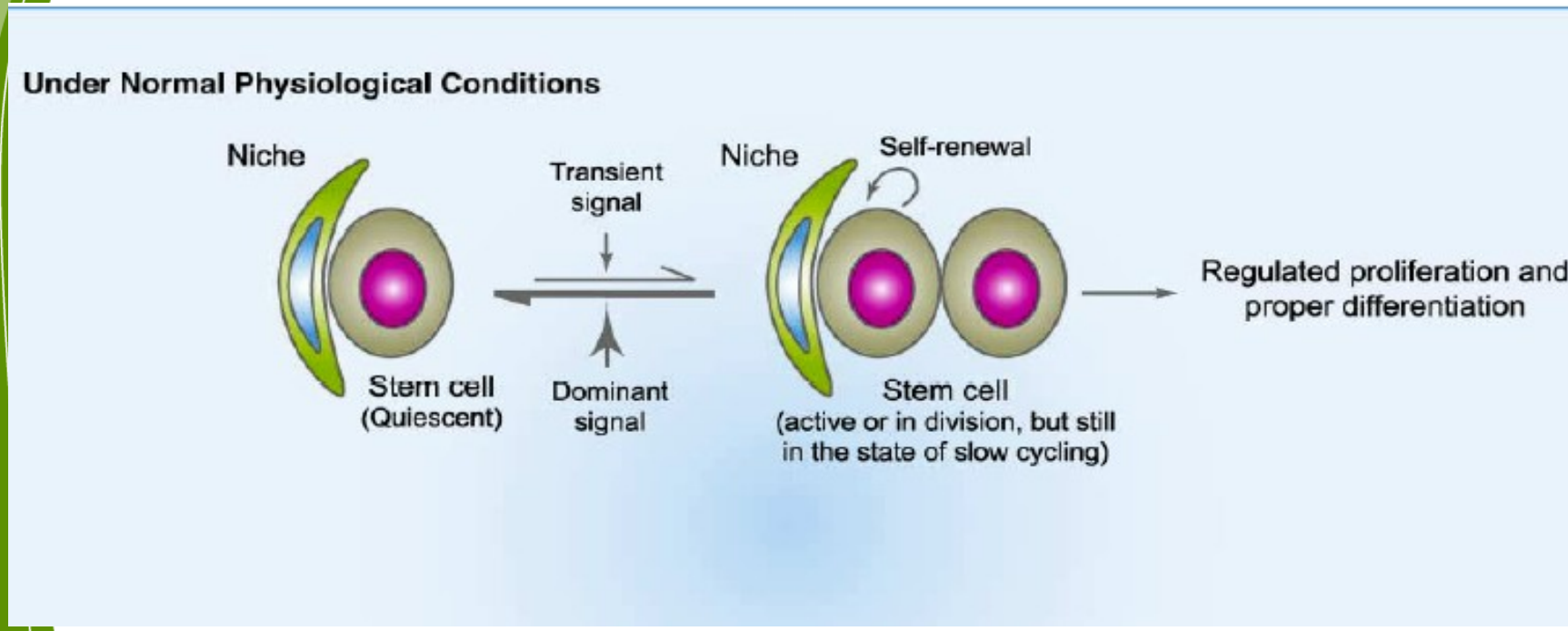

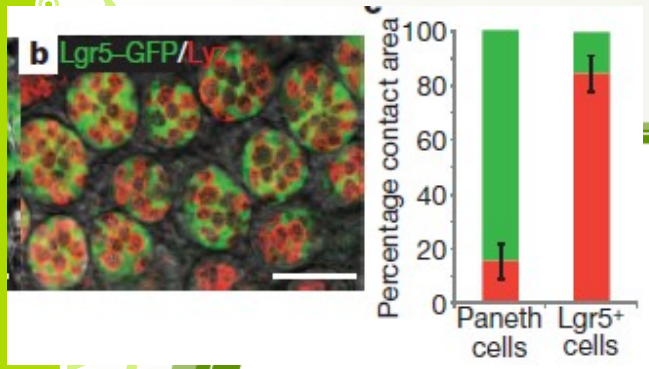

LETTER

doi:10.1038/nature09637

Paneth cells constitute the niche for Lgr5 stem cells in intestinal crypts

Toshiro Sato[1], Johan H. van Es[1], Hugo J. Snippert[1], Daniel E. Stange[1], Robert G. Vries[1], Maaike van den Born[1], Nick Barker[1], Noah F. Shroyer[2], Marc van de Wetering[1] & Hans Clevers[1]

[1]Hubrecht Institute, KNAW and University Medical Center Utrecht, Uppsalalaan 8, 3584CT Utrecht, the Netherlands. [2]Cincinnati Children's Hospital, Division of Gastroenterology, Medical Center, MLC 2010, 3333 Burnet Avenue, Cincinnati, Ohio 45229, USA.

20 JANUARY 2011 | VOL 469 | NATURE | 415

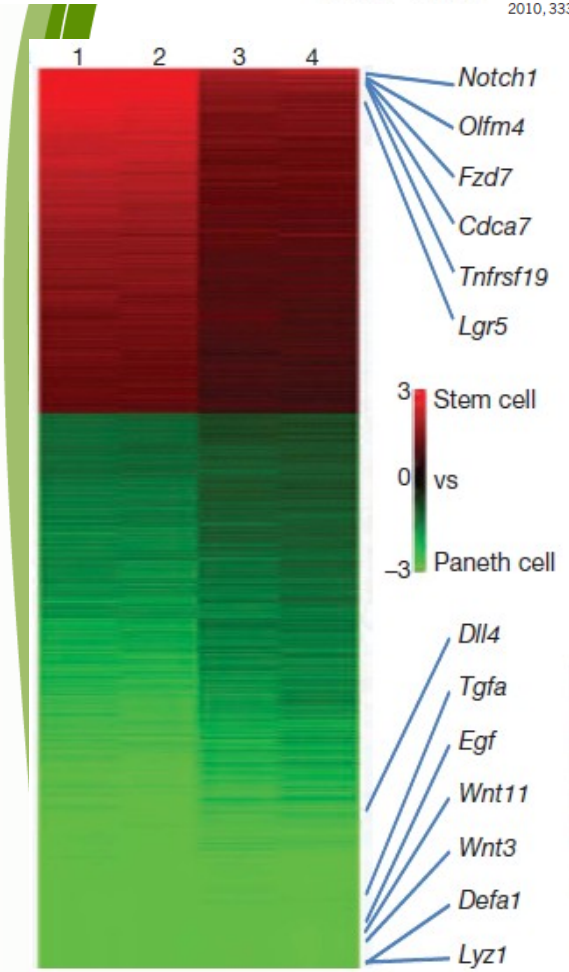

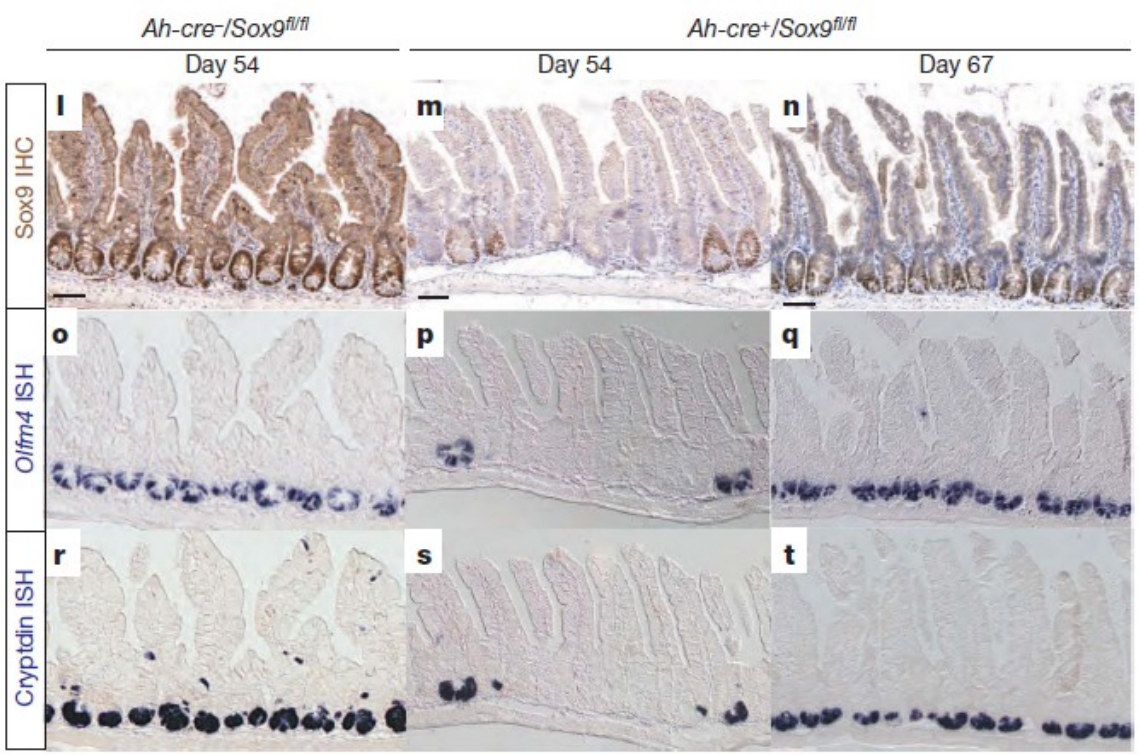

Panetovy buňky jako „niche“ kmenových buněk střeva

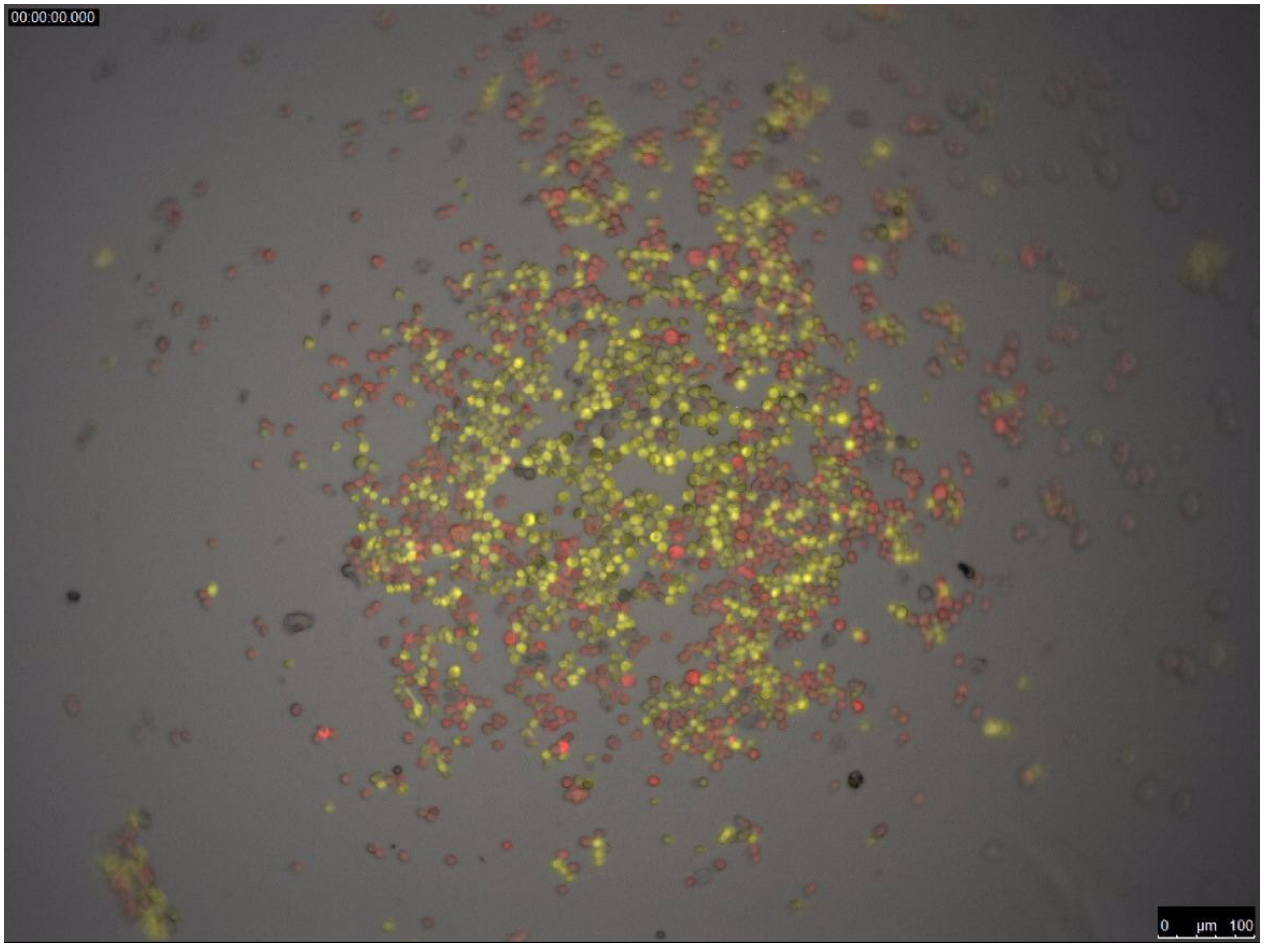

Organoidy

Organoidy

C. Lgr5 pozitivní buňky in vitro dávají vzniknout kompletní villus-crypt struktuře in vitro (Doposud se to s žádnými jinými buňkami nepodařilo)

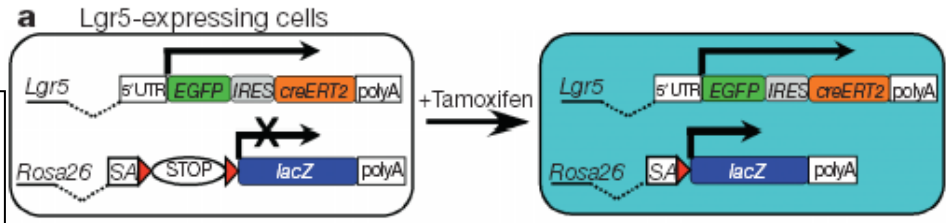

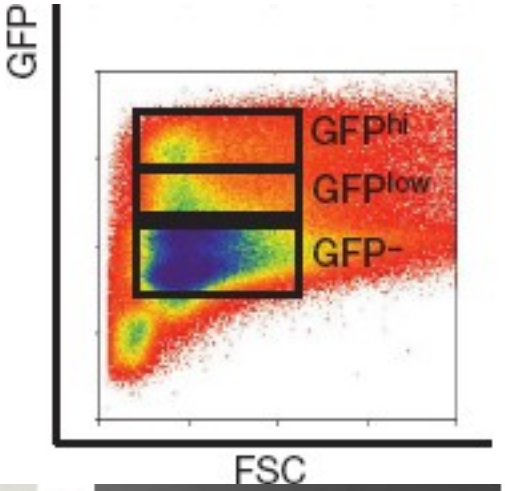

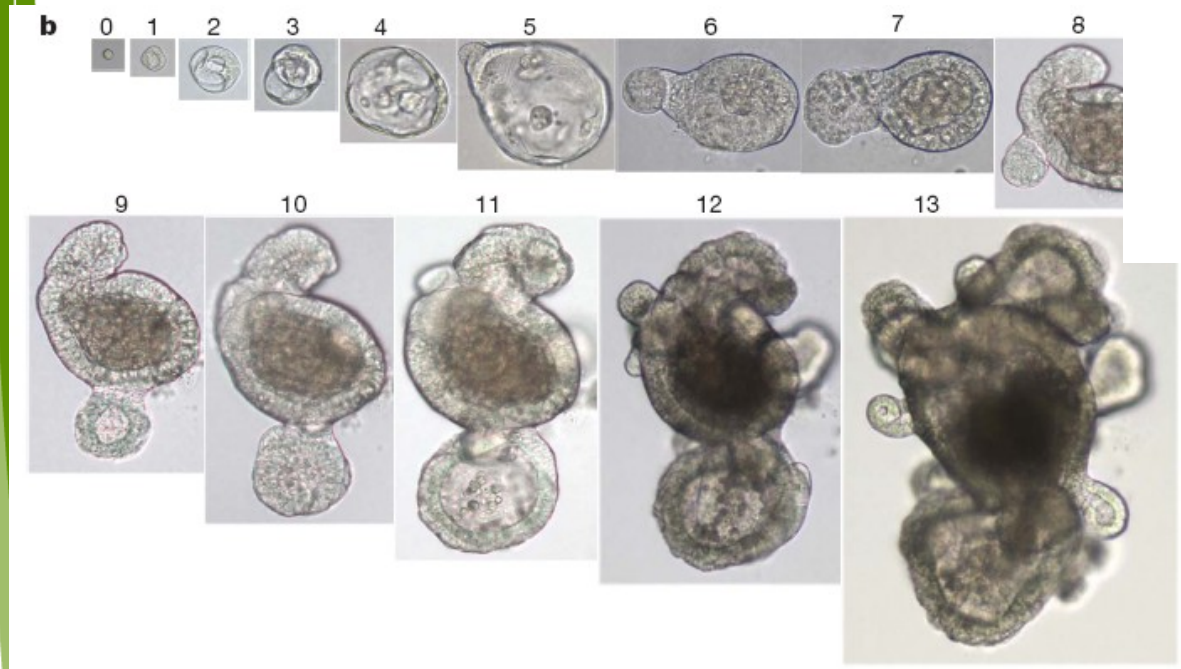

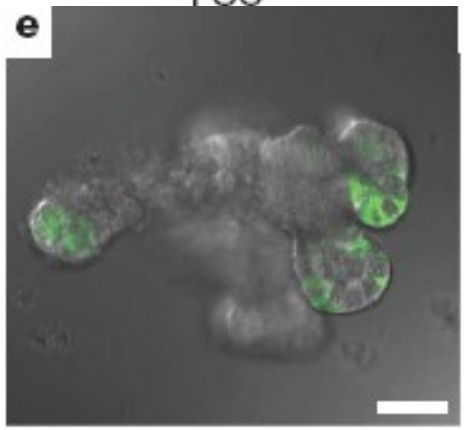

Organoidy

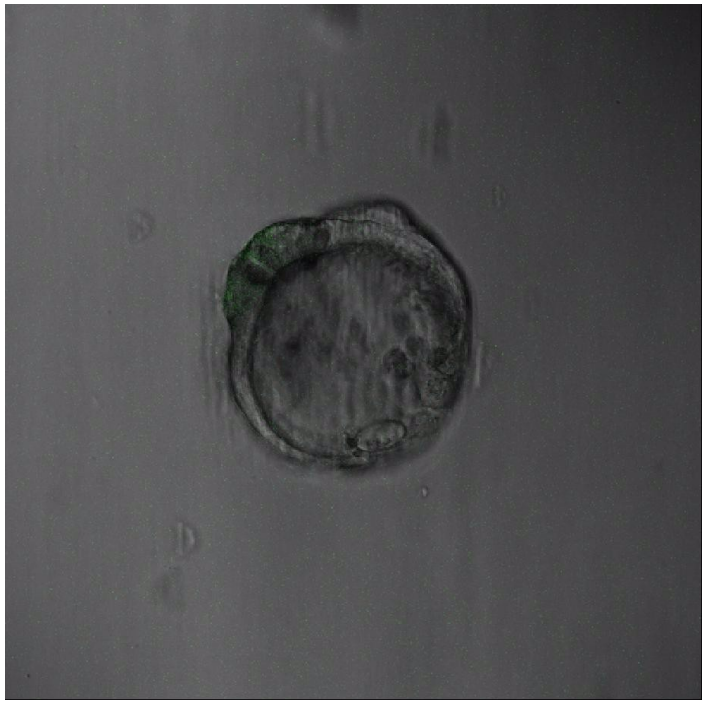

Organoidy

Organoidy

Table 2 Organoid models from various organs and ESCs/iPSCs

Tissue	Source	Organoid morphology	Cell types in organoid	Downstream applications tested	Types of human diseases modelled
Lingual	Mouse lingual stem cells	Spherical and budding organoids	-Stratum corneum -Keratin 5/14+ stem/progenitor cells -Granular cells of intermediate epithelial origin	-Tamoxifen inductions -Lineage tracing -Engraftment studies	Lingual carcinoma
Taste bud	Murine circumvallate tissue	Spherical and budding organoids	-Lgr5+ stem cells -Lgr6+ stem/progenitor cells -UEA/K8+ intragemmal taste bud cells -Gustducin-expressing, T1R3-expressing mature taste receptor cells -Sox9+ proliferative cells in budding regions	-Functional assays -Gene expression analysis -Cell cycle analysis	-
Salivary gland	Primary mouse cells	-Ductal branching organoids -Lobular spherical organoids	-CD24^{hi}/CD29^{hi} stem cells -Cytokeratin 7/18+ duct cells. -Aquaporin5-expressing acinar cells	-Gene expression analysis -Transplantation studies	Hyposalivation
Oesophagus	Mouse/human adult oesophageal tissue	-Spherical multilayered organoids -Human Barrett's oesophagus organoids: budding morphology	-CK14+, p63+ small basal cells in the outer layer, large basal cells in the middle layer, and CK13+ cells in the central keratinized layer -Integrin α_6/β_4^{low} differentiated and integrin α_6/β_4^{hi} stem cells -Barrett's oesophageal organoids express goblet cells following differentiation.	-Tamoxifen inductions -Gene expression analysis	Barrett's oesophagus
Stomach	-Mouse/human adult tissue -Mouse/human ESCs -Human iPSCs	-Pylorus and corpus: spherical organoids -FGF10-driven budding events in pyloric organoids	-Pylorus: Lgr5+ stem cells, mucous neck cells, pit cells, enteroendocrine cells -Corpus: chief cells, mucous neck cells, pit cells	-Microinjection and infection model for *H. pylori* -Transcriptome profiling -Co-culture with mesenchymal cells -Adeno/retroviral transfections	-*H. pylori* infection -Cancer
Intestine	-Adult tissue -Mouse/human ESCs -Human iPSCs	-Normal tissue: branching organoids -Diseased tissue: cystic and other morphologies	-Crypt-like domain contains Lgr5+ stem cells and paneth cells -Villus-like domain harbours villin+ cells -Enteroendocrine and goblet cells scattered throughout organoid	-Transplantation studies -CRISPR/Cas9 gene editing -Cancer mutations -Transcriptome profiling	-Cancer -Cystic fibrosis -Infection model for viral and bacterial infection
Colon	-Adult tissue -Mouse/human iPSCs	-Normal tissue: budding organoids -Diseased tissue: cystic morphologies	-Lgr5+ stem cells -Enteroendocrine cells -Goblet cells -Enterocytes -Lgr5+ stem cells and bile duct cells -Hepatocytes observed after inhibition of Notch	-Transplantation studies -Transcriptome profiling -Biobank	-IBD -Cancer

Organoidy

			& TGF-β pathways		
Liver	-Mouse adult tissue -Human iPSCs	-Mouse organoids: spherical -Human organoids: cystic	-Human organoids contain Lgr5⁺ stem cells, ductal cells and hepatocytes -Cholangiocyte organoids express differentiation markers such as apical sodium-dependent bile acid transporter, secretin receptor, cilia and CFTR.	-Transplantation studies -Transcriptome profiling -Adenoviral transduction -Whole-genome sequencing -CFTR functional assays	-Alagille syndrome -Cystic fibrosis
Pancreas	Mouse/human adult tissue	-E10.5 tissue: branching organoids -Adult tissue: budding organoids	-Ductal organoids contain Lgr5⁺ stem cells -Organoids from E10.5 murine pancreas can be differentiated into exocrine and endocrine cells	-Engraftment studies -Lineage tracing -Adenoviral transduction -Transcriptome profiling	Cancer
Prostate	Mouse/human adult tissue	-Normal tissue: spherical -Diseased tissue: branching similar to morphology of cancerous organoids	-Cytokeratin 5/p63⁺ basal cells -Cytokeratin 8⁺ luminal cells. Lgr4/Lgr5⁺ cells	-Tamoxifen inductions -Lentiviral infections	Cancer
Lung	-Mouse foetal pulmonary cells -Human ESCs/ iPSCs	Spherical organoids	-Uniform proximal Sox2 and distal Sox9 expression -Proximal-like domains included basal, ciliated and club cells that were surrounded by smooth-muscle actin	-Transplantation studies -Cancer mutations -RNA sequencing	Cystic fibrosis
Retina	Mouse ESCs	Spherical organoids	-Outer layer recapitulates retinal pigment -Invaginated layer resembles retinal optic cup containing photoreceptors, ganglion cells, bipolar cells and Muller glia	-	-
Inner ear	Mouse ESCs	Budding organoids	-Functional prosensory vesicles -Otic vesicles also generate functional inner-ear hair cells	-	-
Brain	-Mouse/human ESCs -Human iPSCs -Patient skin fibroblasts	-Early-stage spherical organoids -Later-stage budding organoids	-Early-stage organoids contain continuous neuroepithelia -Cerebral cortical regions contain outer radial glia and cerebral cortical neurons	-Transfection -Transcriptome profiling -Electrical excitation	-Autism -Microcephaly
Kidney	Human iPSCs	-Early-stage spherical organoids -Differentiated stages have budding morphology	Differentiated organoids exhibit segmentation as ducts, tubules and glomeruli	Toxicity screening in response to cisplatin	-

Využití organoidů pro buněčné terapie poruch funkce střeva – např. cystická fibroza

Kmenové buňky střeva (2006)

2006: kmenové buňky definovány jako „label-retaining cells“

- tj. jako buňky, které se nedělí

Co tedy jsou „label-retaining cells“?

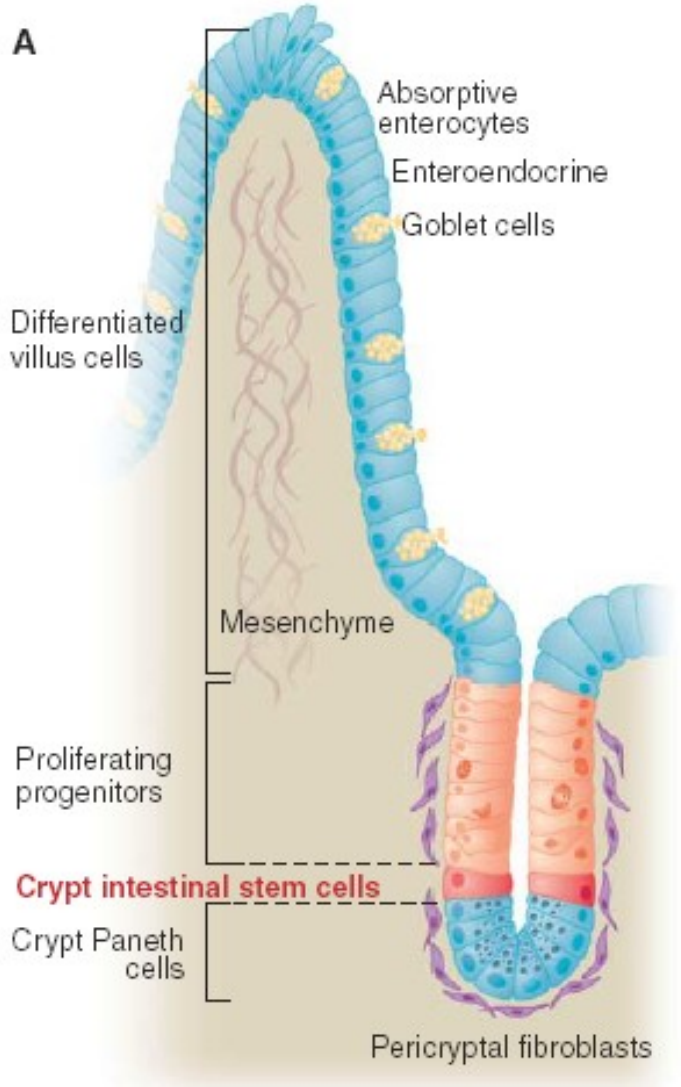

Moore & Lemischka, Science, 2006

Nedělící se zásobárna buněk (Dll1+) pro případ poškození a regenerace:

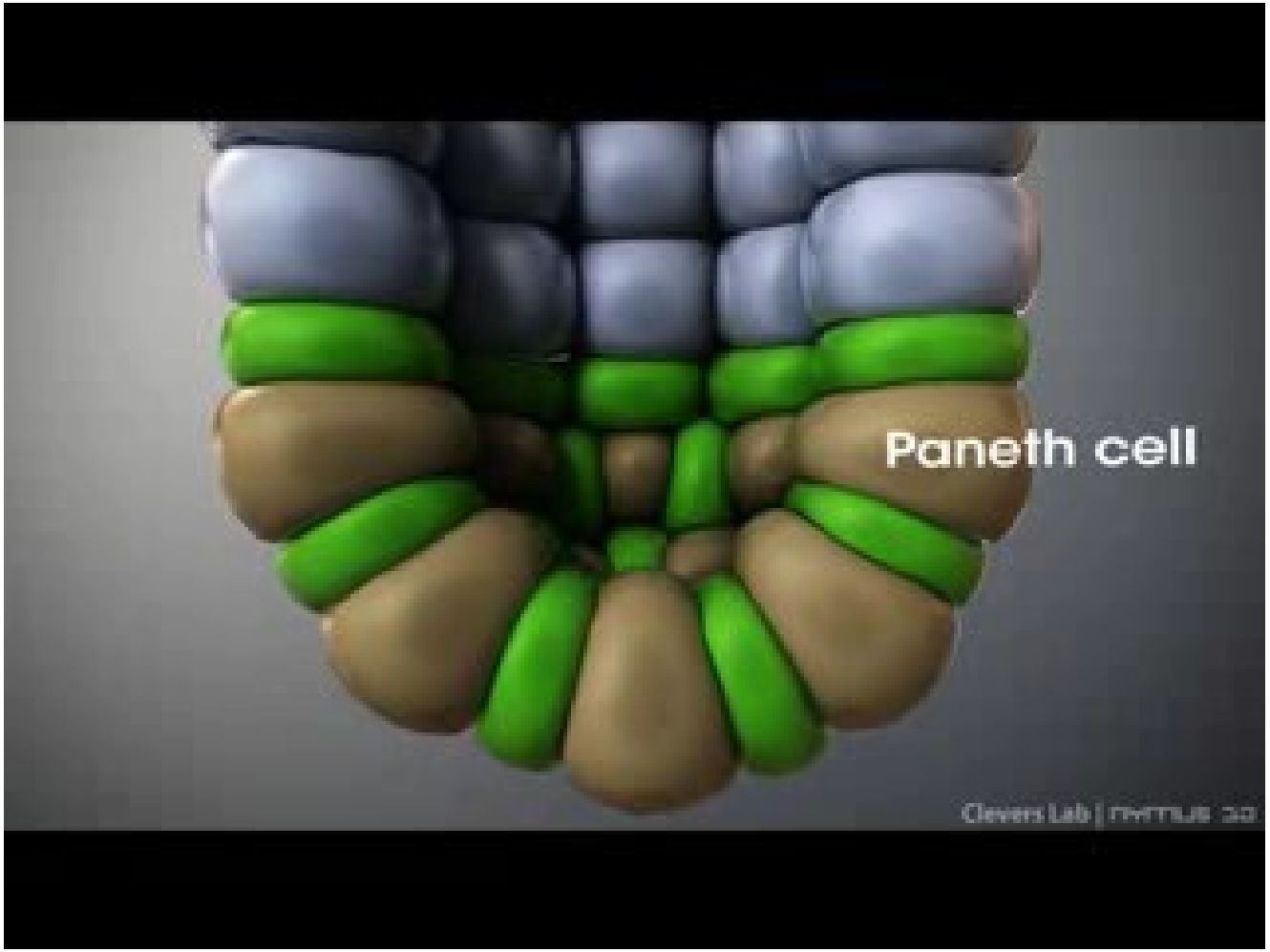

Nedělící se zásobárna buněk pro případ poškození a regenerace:

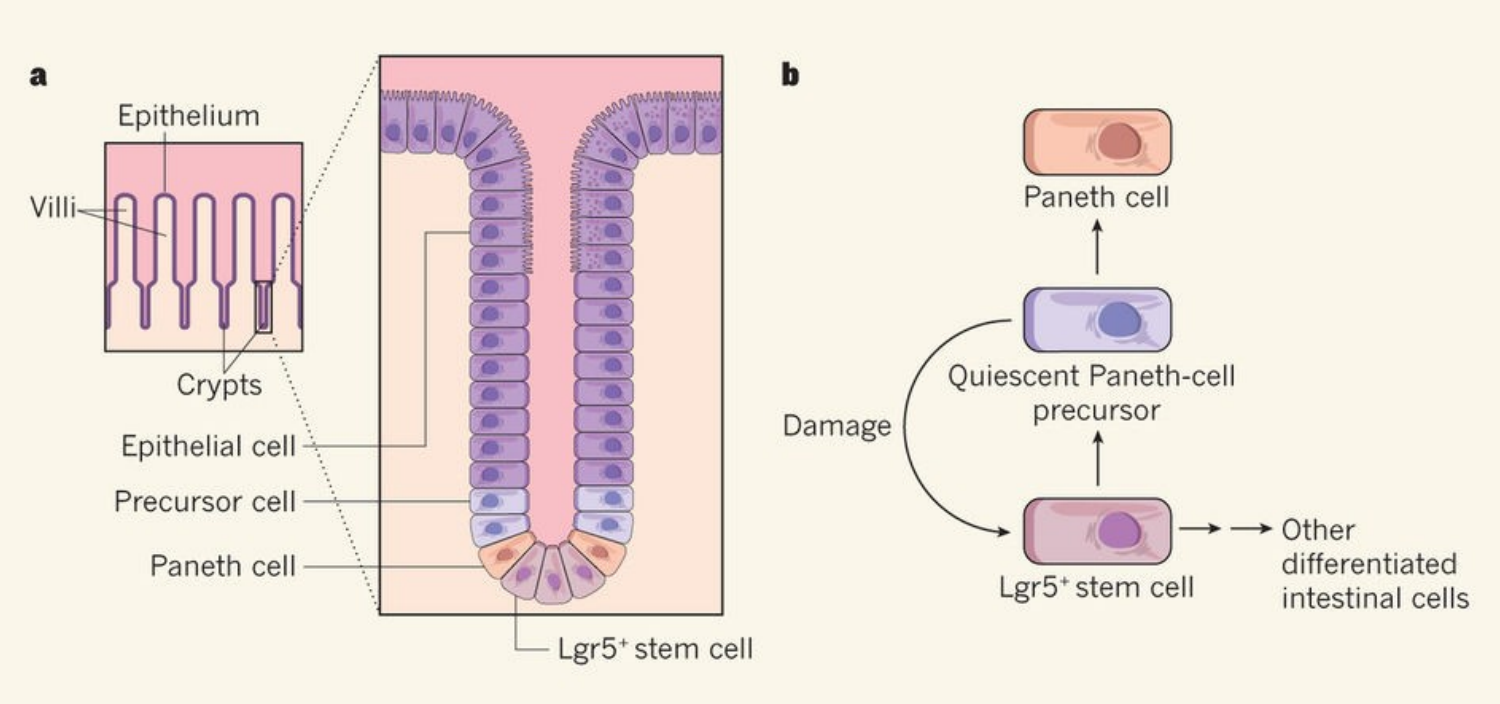

a, The intestinal epithelium follows the distinct contours of villus–crypt units in the intestine. **b**, Normally, Lgr5-expressing stem cells (Lgr5⁺) lead to the production of precursor cells that further differentiate into the various types of crypt epithelial cell. Buczacki *et al.*[1] report that precursors of one type of differentiated intestinal cell, Paneth cells, can persist for several weeks in a quiescent state before maturing into Paneth cells. Intriguingly, these quiescent precursors can revert back into Lgr5⁺ stem cells following crypt damage.

Role kmenových buněk v rozvoji nádoru

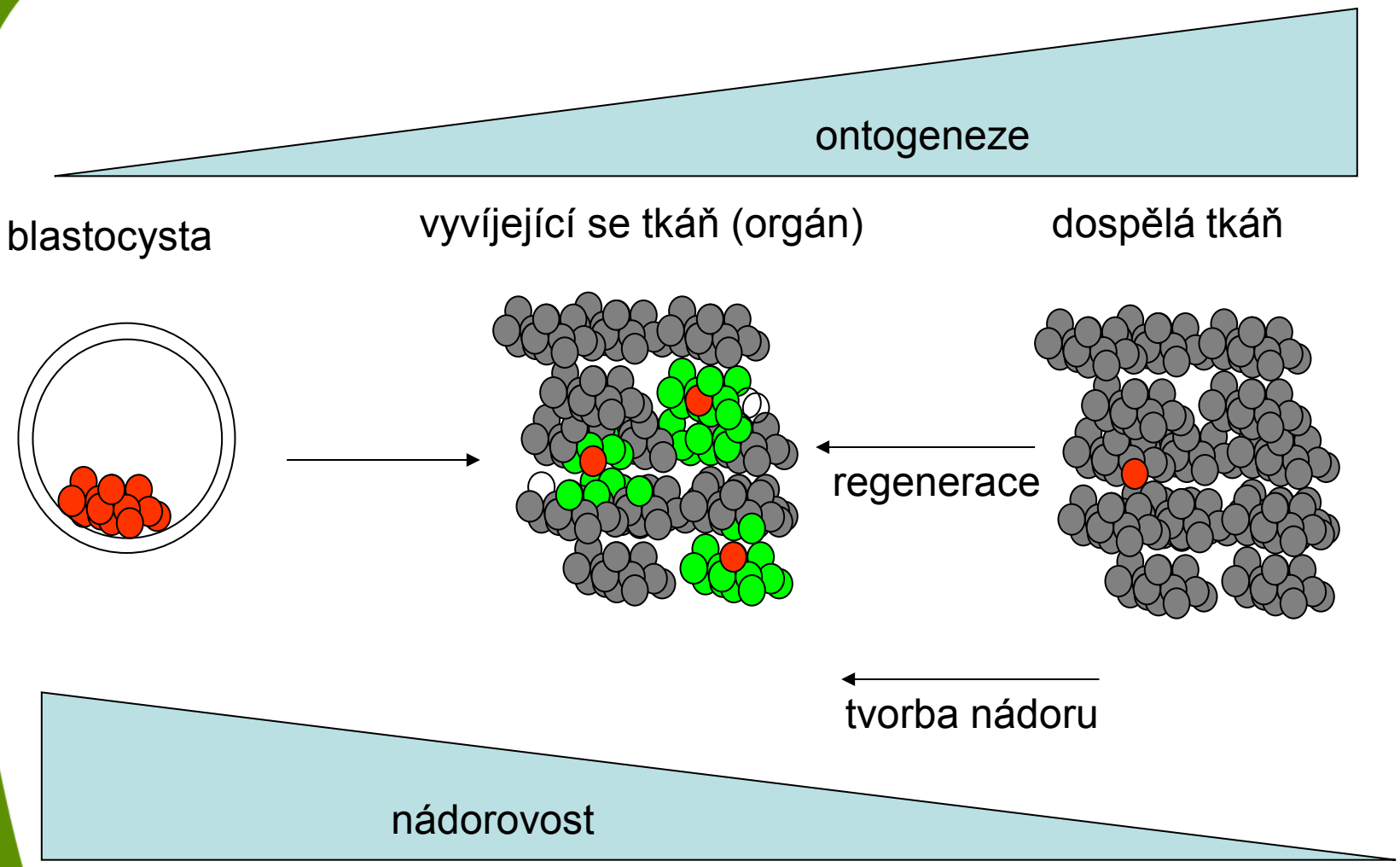

Klasické morfogenetické dráhy (Wnt, Hh, Notch a další) regulují regeneraci, tkáňové specifické kmenové buňky i nádory

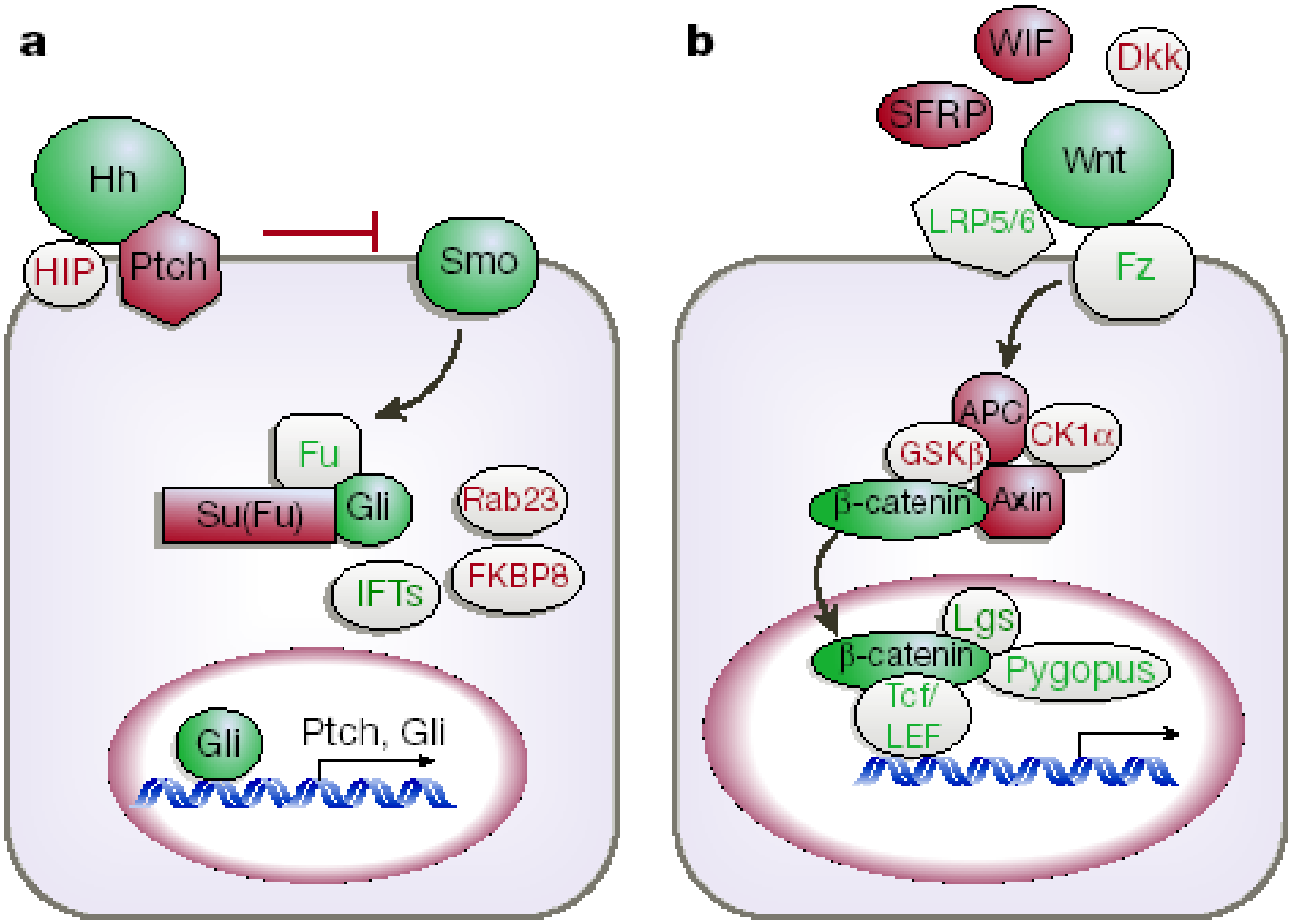

Klasické morfogenetické dráhy (Wnt, Hh, Notch a další) regulují regeneraci, tkáňové specifické kmenové buňky i nádory

- legenda k obrázku:

Figure 1 Hh and Wnt signalling pathways. Simplified views of the Hh and Wnt signalling pathways, with emphasis on components implicated in cancer or tissue regeneration. Green and red colours denote pathway components with primarily positive or negative roles, respectively, in pathway activation. Shaded components have been causally implicated in tumorigenesis (see Table 2 and text; more complete pathway descriptions are available in refs 32–34 for Hh and refs 17, 46 for Wnt). **a**, Activation of the Hh signalling pathway is initiated by binding of a Hh ligand to Ptch. This lifts suppression of Smo, activating a cascade that leads to the nuclear translocation of Gli and the activation of target genes. HIP is a membrane protein that antagonizes pathway activity by binding to Hh ligands, and Fu, Su(Fu), Rab23, FKBP8 and the IFTs (intraflagellar transport proteins) act downstream of Ptch and Smo to regulate Gli. The function of Rab23, FKBP8 and the IFTs outside the CNS is not established. HIP, Hh-interacting protein; Rab23, a member of the Rab family of GTPases; FKBP8, a member of the FK506-binding protein family. **b**, The Wnt signalling pathway is activated by binding of Wnt ligands to their receptors Fz and LRP5/6, leading to the release of β-catenin from the degradation complex and facilitating its entry into the nucleus, where it regulates target gene transcription through association with TcF/LEF, Legless (Lgs) and Pygopus. SFRP, WIF and Dkk are secreted antagonists of Wnt signalling. APC, Axin, GSK3β and CK1a are components of the β-catenin degradation complex. WIF, Wnt inhibitory factor; Dkk, Dickkopf; GSK3β, glycogen synthase kinase 3β; CK1a, casein kinase 1a.

Table 2 **Hh and Wnt pathways in cancer**

Tissue	Tumour	Evidence of pathway involvement	References
Hh pathway			
Brain	Medulloblastoma	Tumorigenesis by inactivation of *PTCH*; allograft and cell-line growth inhibition by cyclopamine; inhibition of autochthonous tumour growth by synthetic small molecule antagonist	37, 81; reviewed in 6
		Tumorigenesis by inactivation of Su(fu)	86
	Glioma	Gli amplification; growth inhibition of some cell lines by cyclopamine	87, 88
Skin	Basal cell carcinoma	Tumorigenesis by inactivation of *PTCH; in vivo* tumorigenesis by expression of activating form of *SMO* or by Shh overexpression and *in vitro* growth inhibition by synthetic Hh pathway antagonist; inhibition of human tumour growth topical cyclopamine	82, 83; reviewed in 6
Muscle	Rhabdomyosarcoma	Tumorigenesis by inactivation of *PTCH*	reviewed in 6
Oesophagus	Adenocarcinoma	Cell-line growth inhibition by cyclopamine, Hh blocking antibody	42
Stomach	Adenocarcinoma	Cell-line growth inhibition by cyclopamine, Hh blocking antibody	42
Pancreas	Adenocarcinoma	Xenograft and cell-line growth inhibition by cyclopamine, Hh blocking antibody; tumour initiation (in mouse) by Shh overexpression	42, 43
Biliary tract	Adenocarcinoma	Xenograft and cell-line growth inhibition by cyclopamine, Hh blocking antibody	42
Lung	Small-cell lung cancer	Xenograft and cell-line growth inhibition by cyclopamine, Hh blocking antibody	41
Prostate	Adenocarcinoma	Xenograft and cell-line growth inhibition and suppression of metastasis by cyclopamine; increased xenograft growth by Shh and Gli overexpression	29, 89, 90
Bladder	Urothelial carcinoma	Increased tumour induction (in mouse) by alkylating agent in *Ptch* heterozygote	91
Oral cavity	Squamous cell cancer	Growth inhibition of cell lines by cyclopamine;	92
Wnt pathway			
Colon	Adenocarcinoma	Tumorigenesis by inactivation of APC, Axin; tumorigenesis by stabilization of β-catenin; epigenetic inactivation of SFRPs	47; reviewed in 45
Liver	Hepatoblastoma	Tumorigenesis (in mouse) by inactivation of APC and by stabilization of β-catenin	reviewed in 45
Blood	Multiple myeloma	Cell-growth inhibition by dominant negative TCF4; growth stimulation by Wnt ligand	93
Hair follicle	Pilomatricoma	Tumorigenesis (in mouse) by overexpression of β-catenin	reviewed in 45
Bone	Osteosarcoma	Dkk3 and LRP5 expression inhibits tumour cell growth *in vitro*	94, 95
Lung	Non-small-cell carcinoma	Apoptosis and cell-growth inhibition by short intefering RNA and a blocking antibody against Wnt2	96
Pleura	Mesothelioma	Apoptosis and cell-growth inhibition by transfection of SFRP	97

Emphasis is placed on functional data showing a requirement for pathway activation in tumour formation and/or tumour cell growth. (See Fig. 1 and text for gene abbreviations.)

Klasické morfogenetické dráhy (Wnt, Hh, Notch a další) regulují regeneraci, tkáňové specifické kmenové buňky i nádory

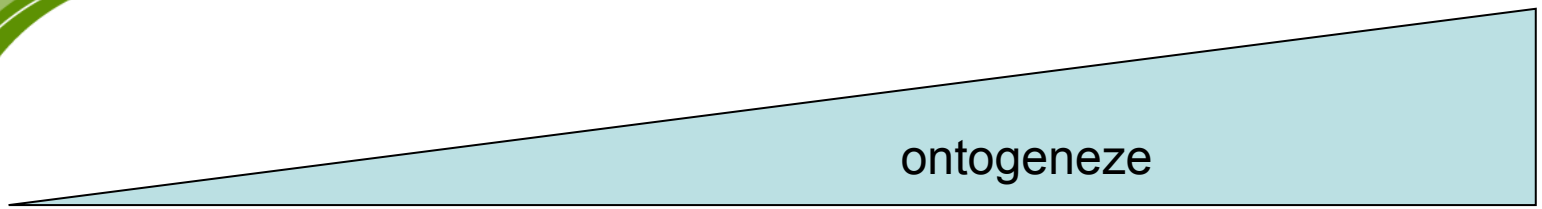

blastocysta

vyvíjející se tkáň (orgán)

dospělá tkáň

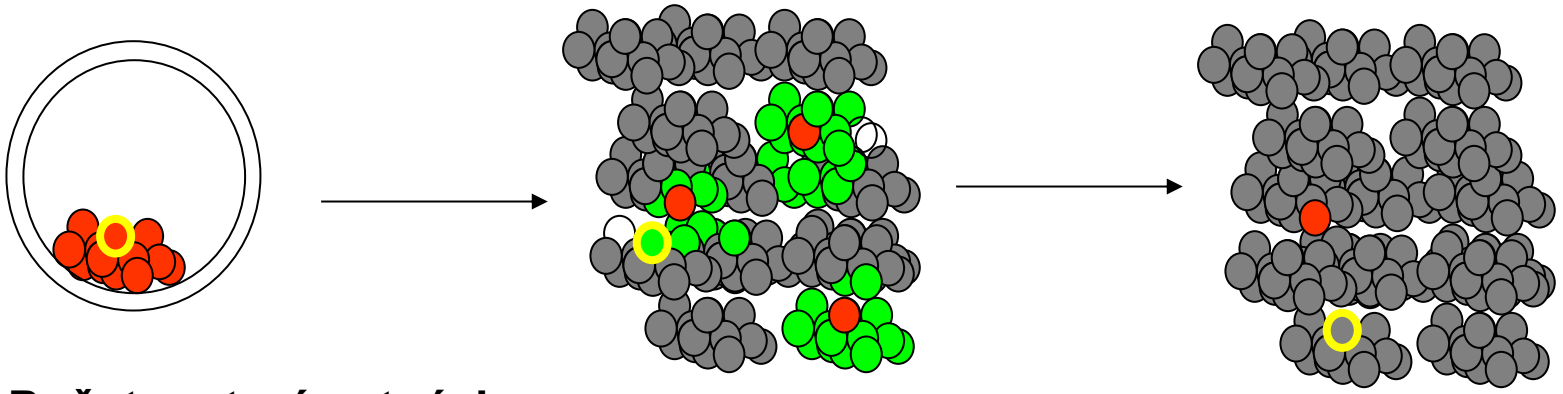

Počet mutací nutných pro vznik nádoru: 0

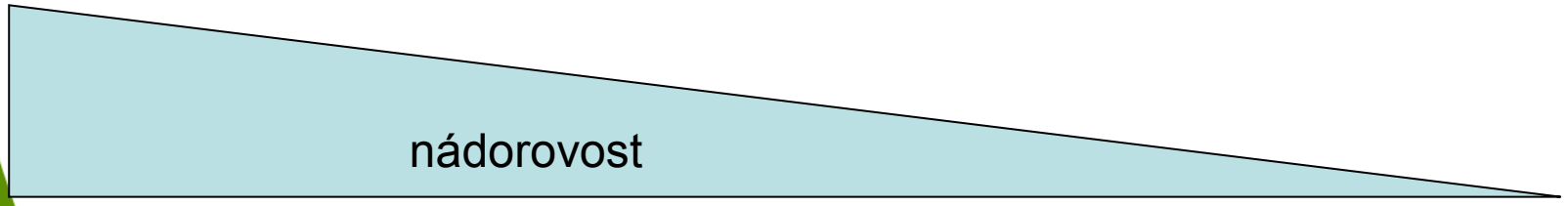

Teratomy

Klasické morfogenetické dráhy (Wnt, Hh, Notch a další) regulují regeneraci, tkáňové specifické kmenové buňky i nádory

Je to pravda?

Experimentální důkaz:

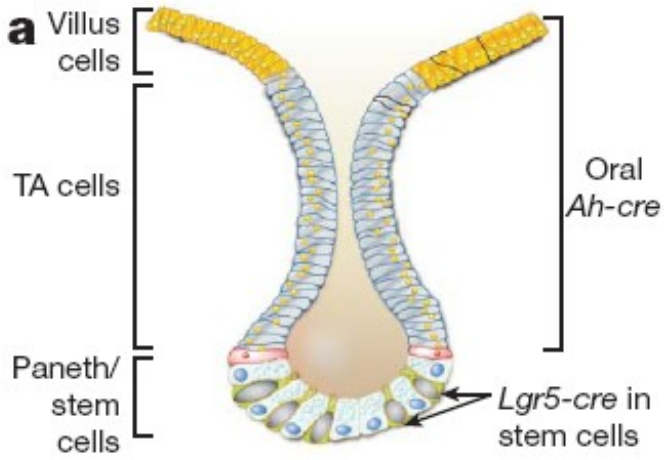

Zkřížení s APC flox/flox myšima + tamoxifen

Vznik malých adenomů, které neprogredují

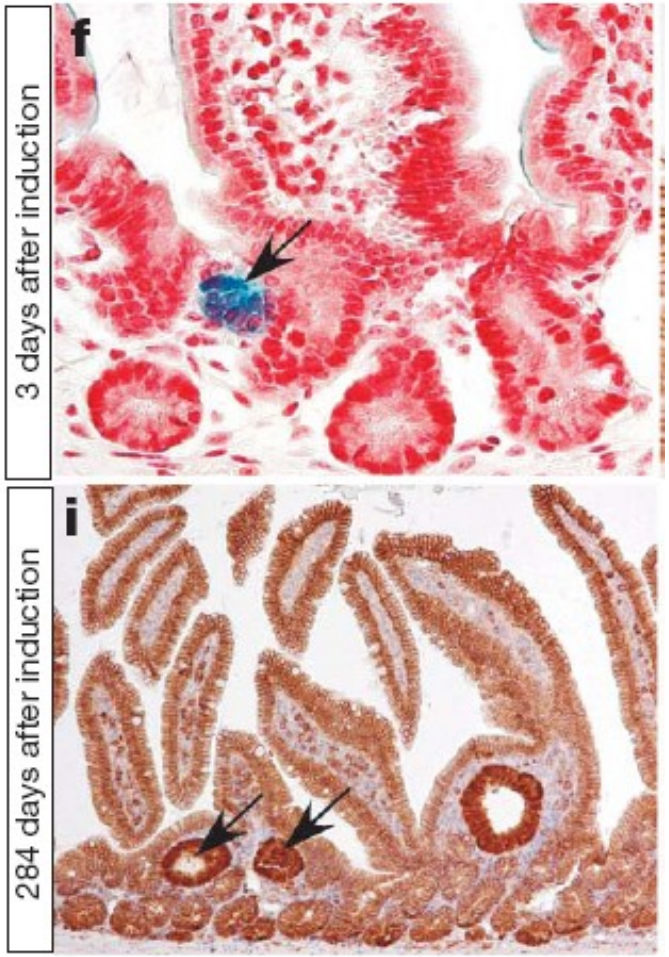

NATURE|Vol 457|29 January 2009

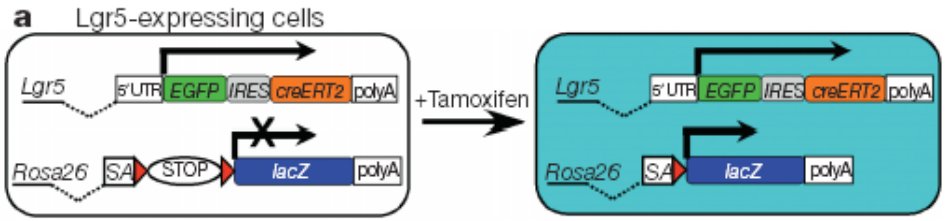

Nekontrolovaná aktivace kmenových buněk má fatální následky

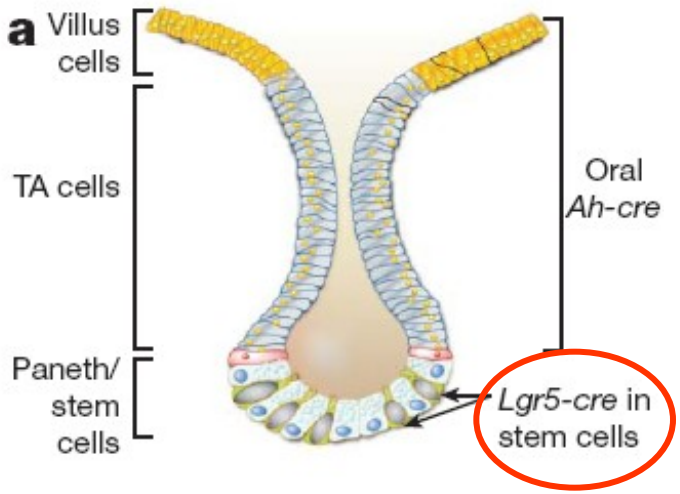

Zkřížení s APC flox/flox myšima + tamoxifen

Rychlý vznik adenomů a nádorů

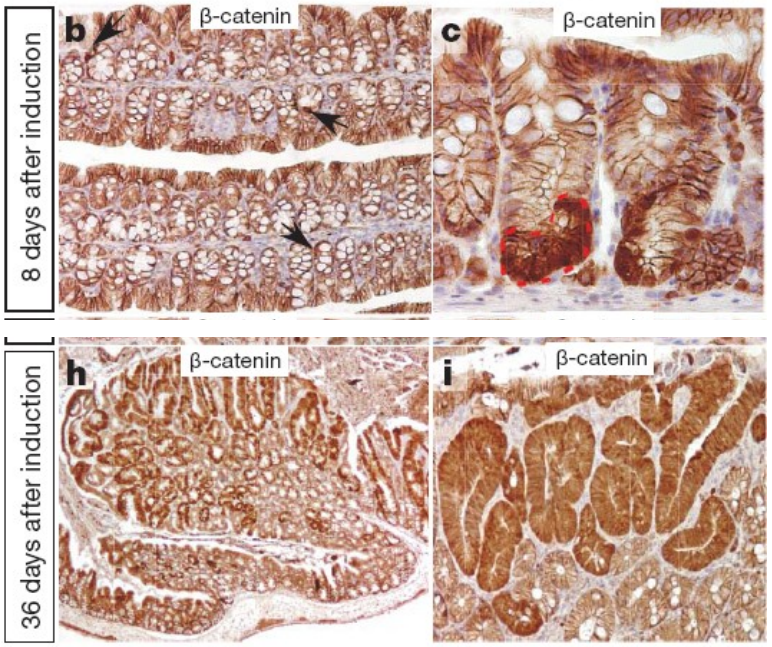

NATURE|Vol 457|29 January 2009

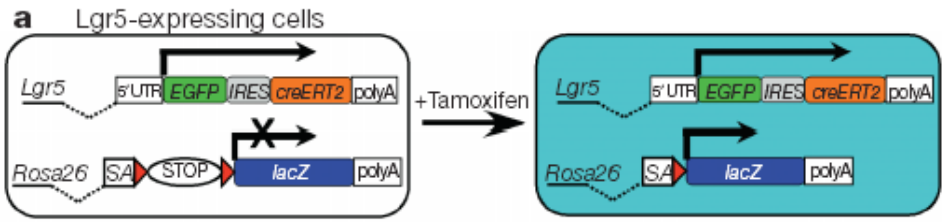

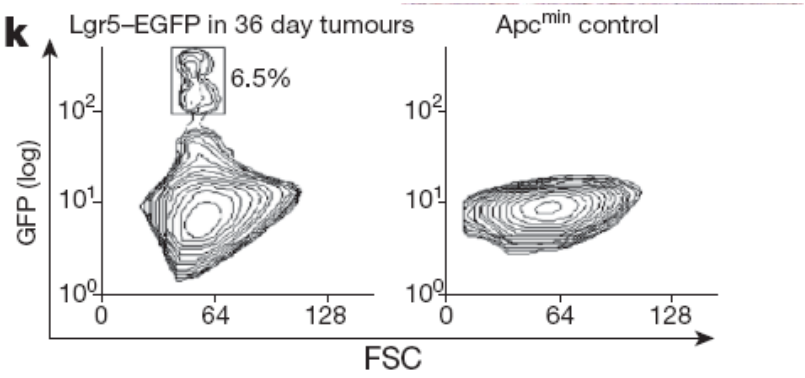

Nádorová kmenová buňka a jejich využití v terapiích

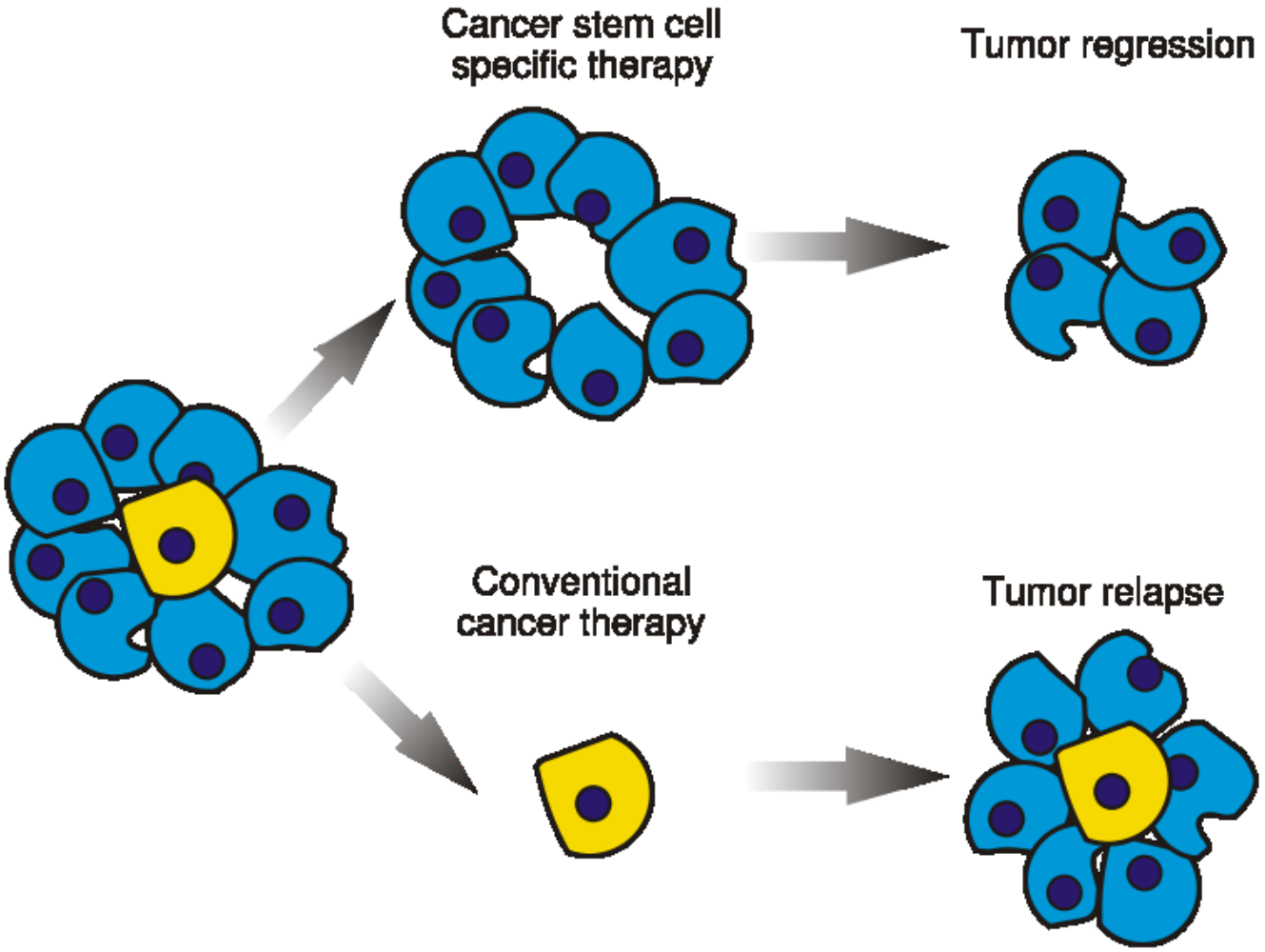

Cancer stem cell based therapy - naděje pro nemocné s nádorem slinivky?

- *Adenokarcinom slinivky - Pancreatic adenocarcinoma* - čtvrtý nejčastější důvod úmrtí u pacientů nádorových onemocnění
- Medián přežití – 4-6 měsí
- 5leté přežití – 1 %
- Léčba gemcitabinem- nez

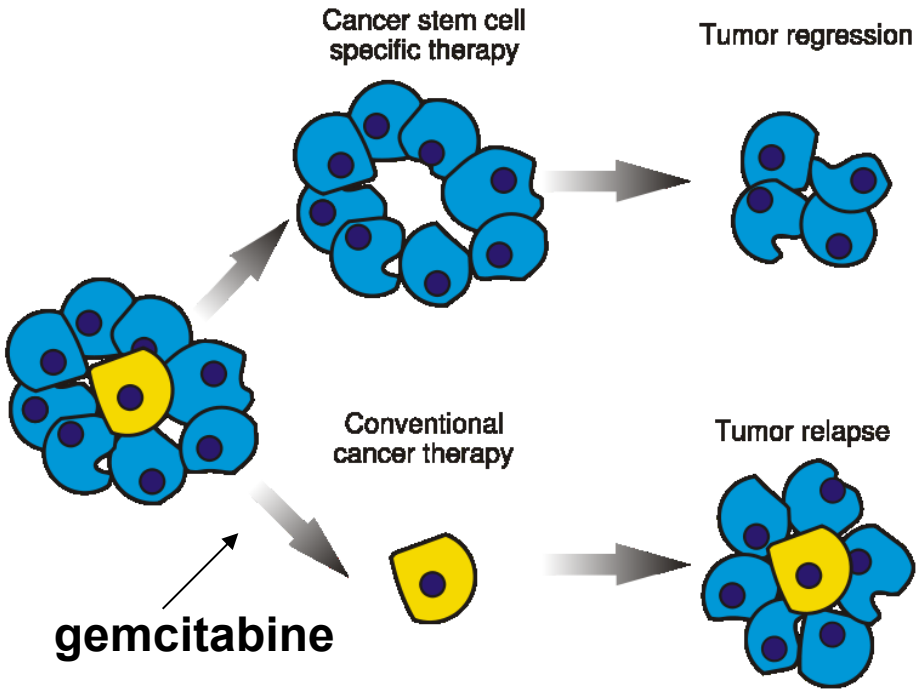

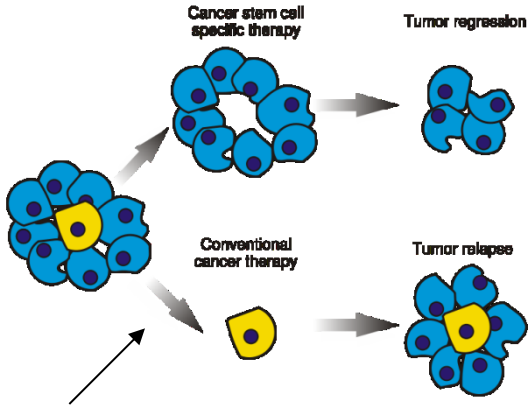

gemcitabine

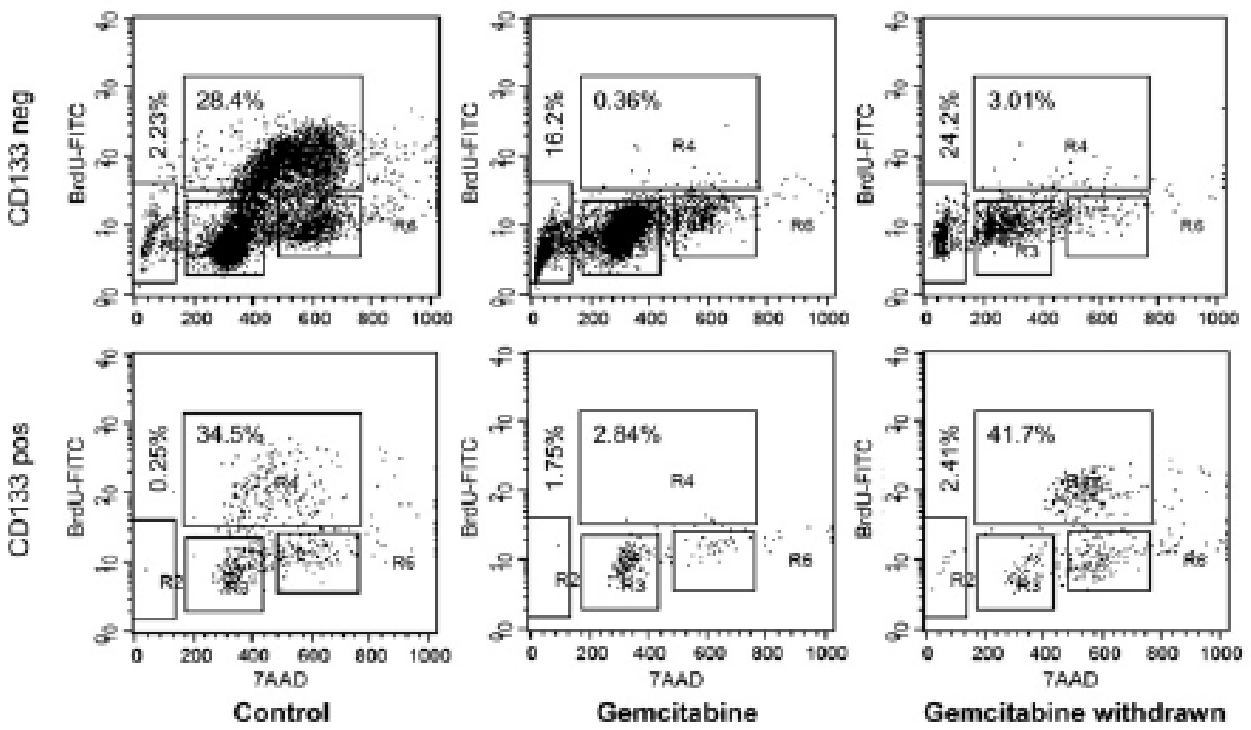

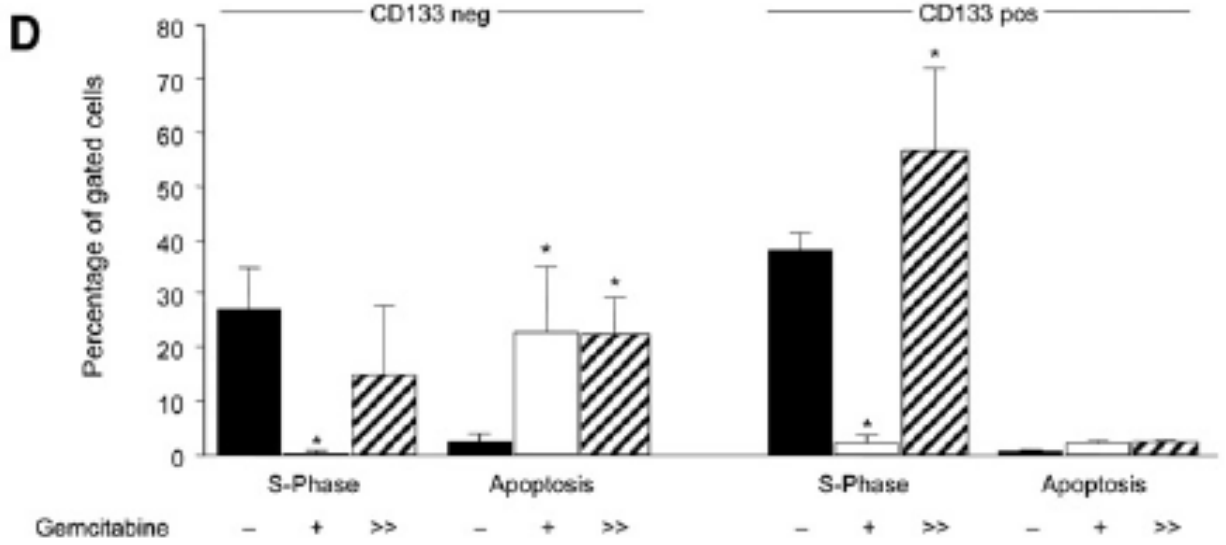

Terapie budoucnosti?

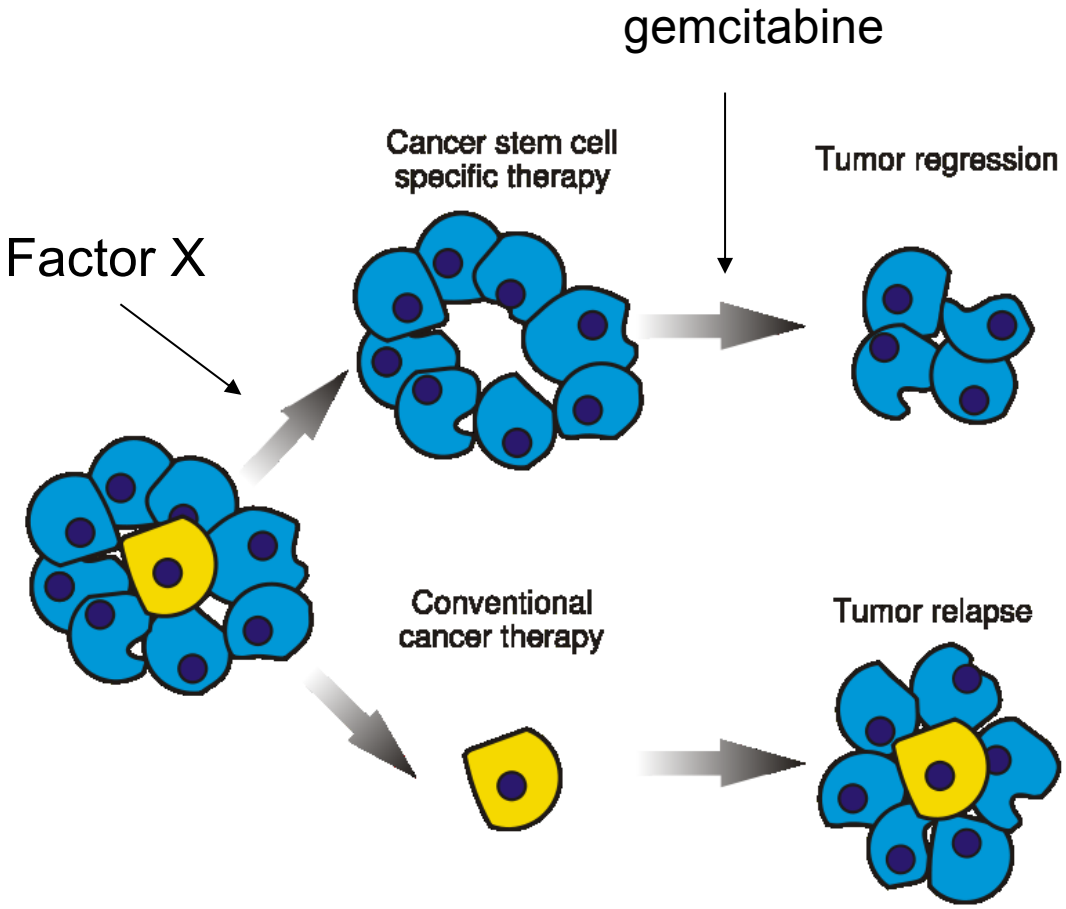

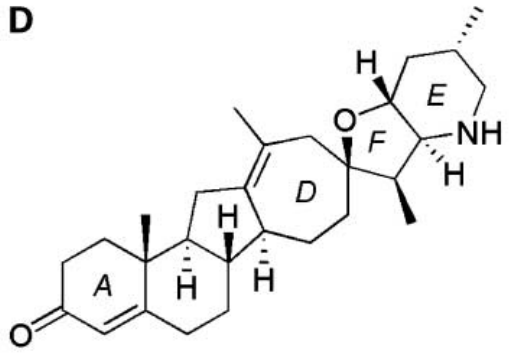

IPI-269609 (IPI-609)

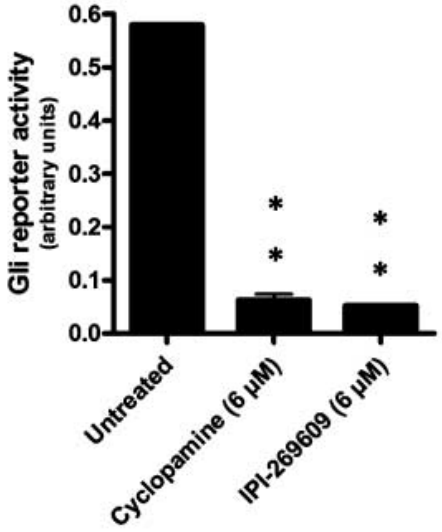

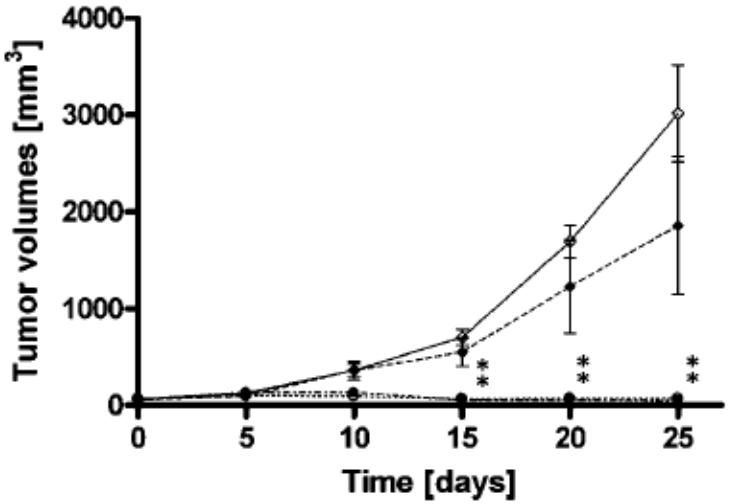

Table 2. Numbers of animals with orthotopic Capan-1 xenografts in which metastases to distant organ sites were found

Group	Control, *n* (%)	IPI-269609, *n* (%)
No. animals	5	5
Lymph nodes	4 of 5 (80)	2 of 5 (40)
Spleen	5 of 5 (100)	0 of 5 (0)
Liver	4 of 5 (80)	0 of 5 (0)
Intestine	5 of 5 (100)	0 of 5 (0)
Lungs	1 of 5 (20)	0 of 5 (0)
Peritoneum	1 of 5 (20)	0 of 5 (0)
Kidneys	1 of 5 (20)	0 of 5 (0)

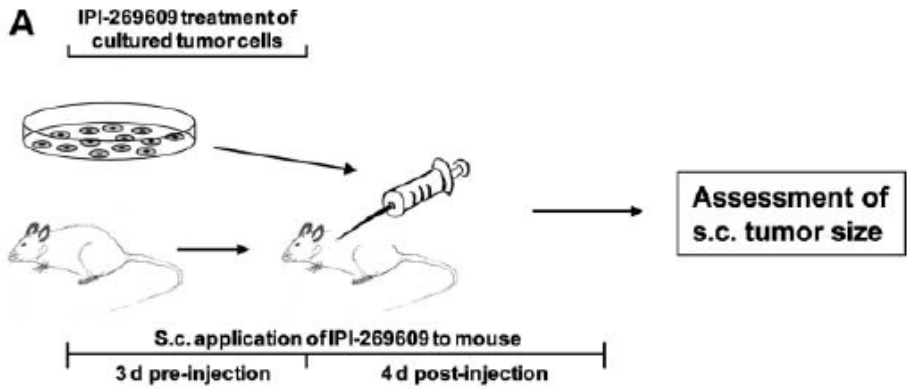

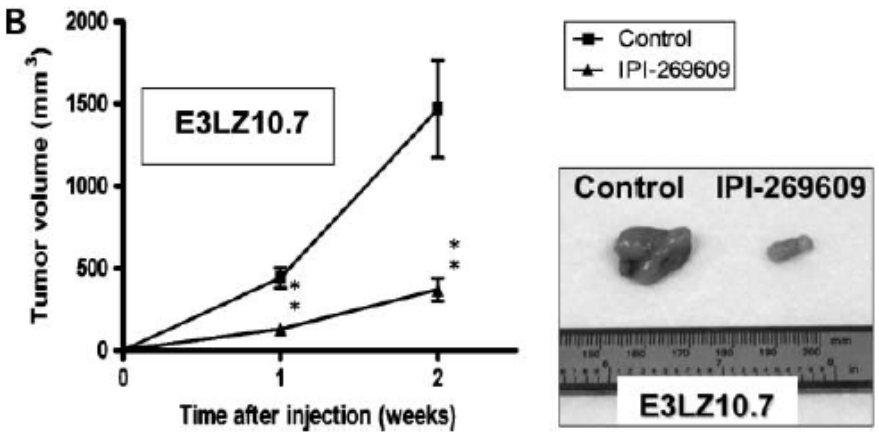

Fyziologie buň. systémů

4 receptors: FGFR1-4
22 ligands: FGF1-23

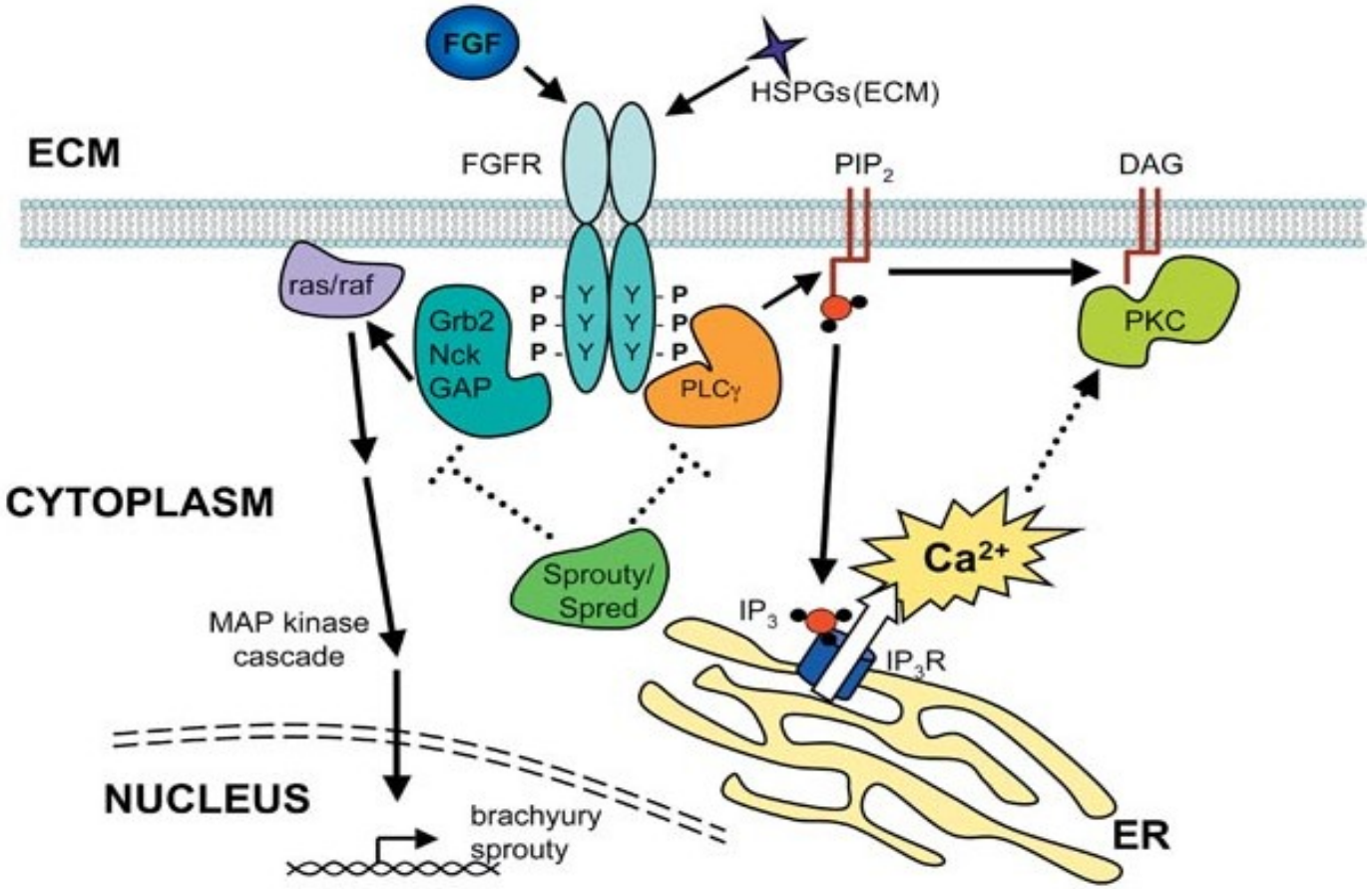

Fyziologie buň. systémů